Bypassing a Highly Unstable Frustrated Lewis Pair: Dihydrogen Cleavage by a Thermally Robust Silylium-Phosphine Adduct

Thomas J. Herrington, Bryan J. Ward, Laurence R. Doyle, Joe McDermott, Andrew J. P. White, Patricia A. Hunt* and Andrew E. Ashley*

Electronic Supplementary Information

Contents

S1 Experimental Details

For the following syntheses the sensitivity towards protic media meant all manipulations were performed inside an MBraun Labmaster DP glove box under a N_2 atmosphere. Solvents were purchased from Sigma Aldrich: PhCl (Anhydrous) and PhF (Anhydrous) were thoroughly dried and distilled over CaH_2; *n*-hexane was dried via filtering through activated alumina, and stored over a K-mirror. Deuterated PhCl (purchased from ABCR) was dried over CaH_2, vacuum distilled, and finally freeze-thaw degassed. Trisopropylsilane (Sigma-Aldrich, 99%) was used as supplied. tBu$_3$P[1] and [Ph$_3$C][B(C$_6$F$_5$)$_4$][2] were prepared according to literature preparations. H_2 (5.5 Research Grade BOC) was dried *via* passage through a WA-500 OMX drying column purchased from Matheson NANOCHEM®. D_2 (99.8% Cambridge Isotope Laboratories) was dried *via* passage through a Supelpure-O® Oxygen/Moisture Trap. To prevent protonation from glassware, all reactions were performed in Teflon® vials (see S11) with NMR experiments recorded in tubes containing Teflon® inserts (Norell NMR-100-520D), except those requiring a glass capillary insert for referencing ^{31}P NMR spectra (e.g. PPh$_3$/C$_6$D$_5$Cl; Figure 7).

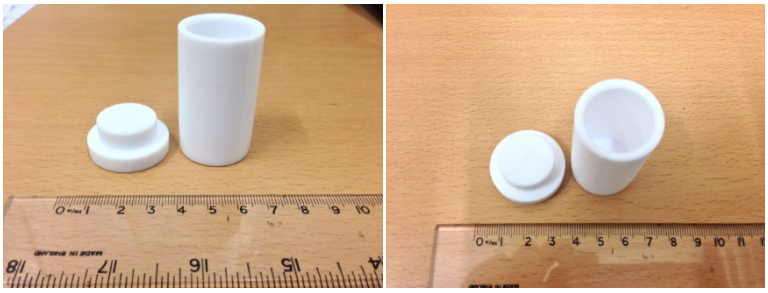

Figure 1. Side and top views of Teflon® vials used in the synthesis of **1**.

NMR spectra were recorded using Bruker AV-400 (400 MHz) and AV-500 (500 MHz) spectrometers. Chemical shifts, δ, are reported in parts per million (ppm). ^{1}H and ^{13}C{^{1}H} chemical shifts are given relative to Me$_4$Si and referenced internally to the residual proton shift of the deuterated solvent employed. ^{19}F, ^{31}P{^{1}H} and ^{29}Si chemical shifts were referenced externally to $CFCl_3$, 85% $H_3PO_{4(aq)}$ and Me$_4$Si, respectively. All samples were prepared inside a glovebox using NMR tubes fitted with J. Youngs valves and contained Teflon® inserts. In preparation for quantitative ^{1}H and ^{31}P NMR data, T_1 measurements were determined using an inverse-recovery experiment ([tBu$_3$PH]$^+$ = 3.2 s and **1** = 10 s). ^{31}P NMR spectra were measured using an inverse gated acquisition with a relaxation delay of 70 s and excitation pulse of 30° (to avoid NOE build-up). The sweep width of 400 ppm (190 to –210 ppm) was acquired using 64K data points, resulting in an acquisition time of 0.51 s. Shorter

relaxation delays were found to deliver a higher relative phosphonium to adduct ratio in both ^{1}H and ^{31}P NMR experiments.

High resolution mass spectrometry samples (HRMS ESI) were recorded using a Micromass LCT Premier spectrometer, using PhF solvent.

IR spectra were recorded on a Perkin Elmer GX FT-IR spectrometer (range 4000-400 cm^{-1}, resolution 0.5 cm^{-1}) using KBr pellets.

Elemental analysis was conducted by Mr. S. Boyer of the London Metropolitan University.

S2 X-ray Crystallographic Details

The absence of any disorder in the structure of **1** allowed for confident assignment of the silicon and phosphorus centres. Additionally, when the element identities were deliberately swapped the final *R*-factor rose from 0.0354 to 0.0382, the thermal parameters of the two atoms become more disparate, and a noticeable hole in the final ΔF map of 0.63 $eÅ^{-3}$ was found only *ca*. 0.3 Å away from the silicon site (consistent with the over-assignment of electron density when it was being modelled as phosphorus).

S3 Synthesis of [*t*Bu$_3$P–Si*i*Pr$_3$][B(C$_6$F$_5$)$_4$] (1)

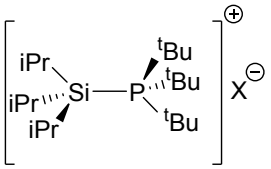

X = B(C$_6$F$_5$)$_4$

Inside a glove-box, 1.6 equivalents *i*Pr$_3$SiH (0.110 g, 0.69 mmol) was added to a Teflon® vial containing a stirred orange slurry of [Ph$_3$C][B(C$_6$F$_5$)$_4$] (0.400 g, 0.43 mmol) in PhCl (2 ml), at room temperature. Over 5 minutes the solution decolourised, at which point 1.2 equivalents *t*Bu$_3$P (0.105 g, 0.52 mmol) was added. After the solution was stirred for a further 5 minutes, addition of hexane (3 ml) led to formation of a white precipitate. The solid was left to settle and the supernatant siphoned off via syringe. To guarantee removal of trace *t*Bu$_3$P and Ph$_3$CH, the solid was washed thoroughly with hexane (3 x 10 ml), and dried under vacuum to yield a white powder. Recrystallization of this product from PhCl (–25ºC) produced

microcrystalline **1**, which was washed with hexane (2 x 3 ml) and dried in vacuo (0.400 g, 89%, 0.39 mmol). Crystals suitable for X-ray crystallography were grown by cooling a concentrated PhF solution, from room temperature to –25ºC, within a glove-box freezer. **^{1}H NMR** (400.4 MHz, C_6D_5Cl, 25 ºC) δ: 1.01 (d, $^{3}J_{HH}$ = 6 Hz, 18H, $[(CH_3)_2CH)]_3Si$), 1.13 (d, $^{3}J_{HP}$ = 14 Hz, 27H, $[(CH_3)_3C]_3P$), 1.40 (m, 3H, $[(CH_3)_2CH]_3Si$). **^{13}C{^{1}H} NMR** (125.8 MHz, C_6D_5Cl, 25 ºC) δ: 17.0 (d, $^{2}J_{CP}$ = 7 Hz, $[(CH_3)_2CH]_3Si–P$; d, $^{1}J_{C^{29}Si}$ (ca. 5%) = 50 Hz, $[(CH_3)_2CH]_3{}^{29}Si–P$), 20.4 (s, $[(CH_3)_2CH]_3Si–P$), 31.7 (br s, $[(CH_3)_3C]_3P$), 41.1 (d, $^{1}J_{CP}$ = 10 Hz, $[(CH_3)_3C]_3P$), 136.8 (dm, $B(C_6F_5)_4$, $^{1}J_{CF}$ = 240 Hz, *m*-CF), 138.8 (dm, $B(C_6F_5)_4$, $^{1}J_{CF}$ = 235 Hz, *p*-CF), 148.9 (dm, $B(C_6F_5)_4$, $^{1}J_{CF}$ = 240 Hz, *o*-CF). **^{31}P{^{1}H} NMR** (162.1 MHz, C_6D_5Cl, 25 ºC) δ: 57.3 (s). **^{29}Si NMR** (99.4 MHz, C_6D_5Cl, 25 ºC) δ: 43.1 (d, $^{1}J_{SiP}$ = 23 Hz). **^{19}F NMR** (376.8 MHz, C_6D_5Cl, 25 ºC) δ: –166.1 (m, $B(C_6F_5)_4$, *m*–CF), –162.3 (t, $B(C_6F_5)_4$, $^{3}J_{FF}$ = 21 Hz, *p*–CF), –131.6 (d, $B(C_6F_5)_4$, $^{3}J_{FF}$ = 17 Hz, *o*–CF). **IR** (KBr, cm^{-1}): 1644 (s), 1515 (s), 1463 (s), 1402 (s), 1376 (s), 1329 (w), 1276 (s), 1163 (s), 1086 (s), 1024 (m), 980 (s). **HRMS (ES+, *m*/z)**: for $[C_{21}H_{49}SiP]^+$ Calcd: 360.3341 Found: 360.3344. **HRMS (ES–, *m*/z)**: for $[BC_{24}F_{20}]^-$ Calcd: 679.9852 Found: 679.9854. **Anal** Calcd for $C_{45}H_{48}BF_{20}PSi$: C, 52.03; H, 4.66. Found: C, 51.84; H, 4.47.

S4 General Procedure for H_2/D_2 Activation Experiments.

1 proved to be highly reactive to even trace amounts of H_2O, hence NMR experiments were performed in Teflon® inserts. Reactions in dilute solution, such as those under H_2, invariably become exposed to trace amounts of H_2O (especially as an impurity in H_2 gas), leading to $[t\text{Bu}_3\text{PH}]^+[B(C_6F_5)_4]^-$ and $(i\text{Pr}_3\text{Si})_2O$ (2:1); hydrolysis thus produces twice the amount of phosphonium salt than the reaction with H_2.

Inside a glove-box, 20mg (0.02 mmol) of **1** was dissolved in C_6D_5Cl and transferred to a J Young sealed NMR tube containing a Teflon® insert. The solution was then measured by both ^{31}P and ^{1}H NMR to confirm the integrity of the adduct relative to any $t\text{Bu}_3\text{P}–H^+$ impurity, which would result from partial hydrolysis. The solution was degassed once using the freeze-thaw method and sealed under 1 bar pressure of H_2 at 77 K (to ensure reproducible pressures all tubes were immersed in liquid N_2 to a control depth of 10 cm and backfilled for 10 s); this results in an equivalent internal NMR tube pressure of *ca.* 4 bar at room temperature. ^{31}P and ^{1}H NMR spectra of the solution were subsequently recorded again to ascertain the contribution from adventitious moisture (from H_2 gas) to the $t\text{Bu}_3\text{P}–H^+$ signal. The tube was then immersed in an oil bath (control depth 10 cm) and heated at 90°C. Reaction was complete after 8 hours, as judged by ^{31}P and ^{1}H NMR spectroscopy. The yield for H_2 conversion is most reliably calculated via relative integration of ^{1}H NMR signals for

the iPr_3SiH resonance against that of tBu_3PH (1:1 from H_2). This experiment was repeated a further 3 times to give a H_2 heterolysis yield of 90–94%, calculated on the basis of the initial amount of **1**.

S5 ^{1}H, $^{13}C\{^{1}H\}$, $^{31}P\{^{1}H\}$, ^{29}Si and ^{19}F NMR data for 1

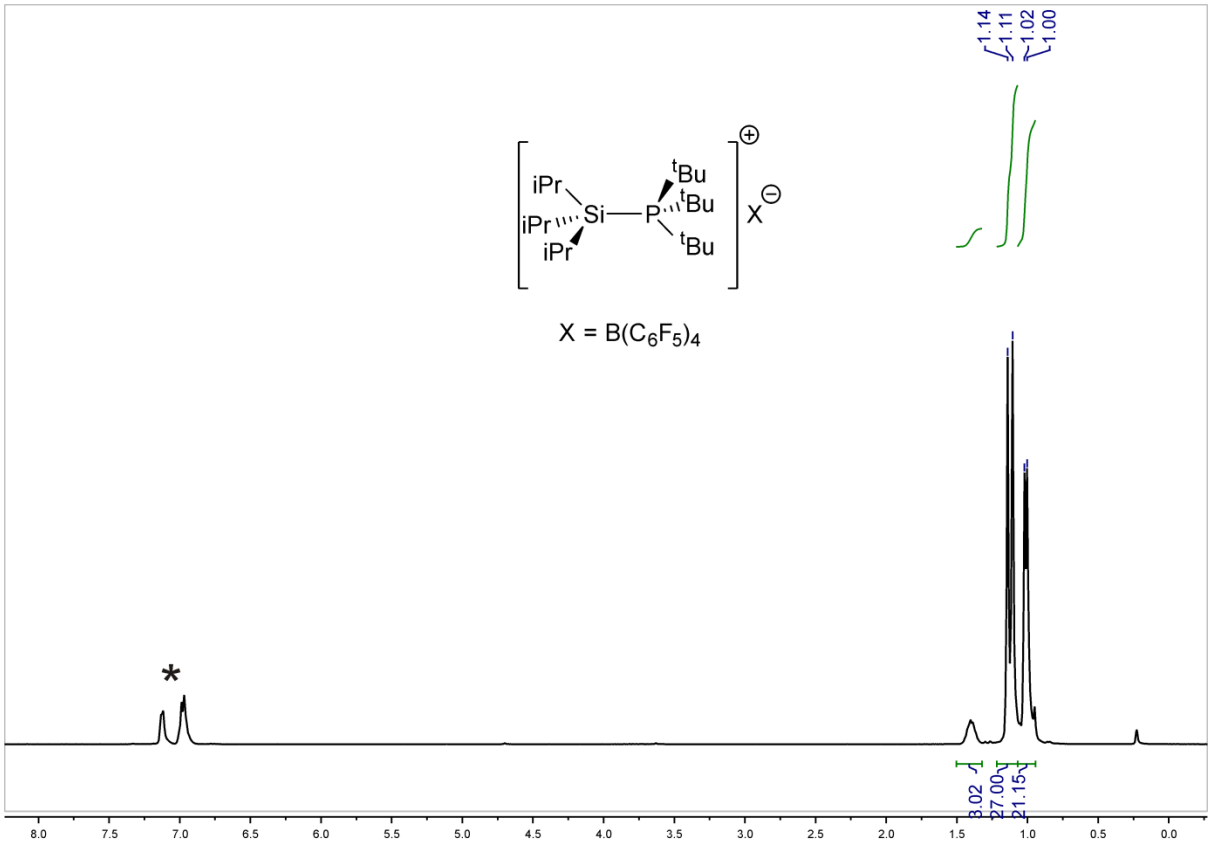

Figure 2. ^{1}H NMR spectrum of **1** in C_6D_5Cl solvent. * denotes resonances attributed to residual protio-solvent.

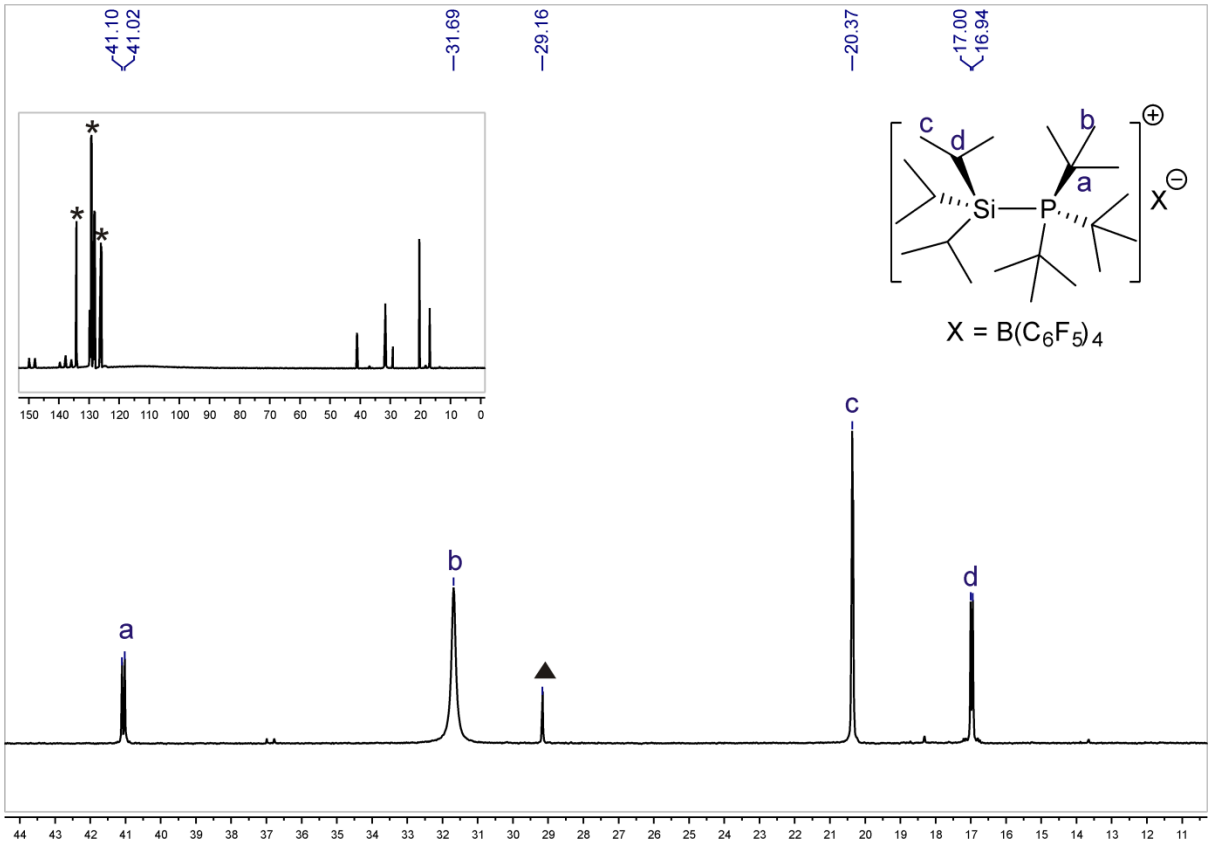

Figure 3. ^{13}C NMR spectrum of **1** in C_6D_5Cl solvent. ▲denotes trace [tBu$_3$PH][B(C_6F_5)$_4$] (due to adventitious H_2O). Inset displays full spectrum, solvent resonances denoted by *.

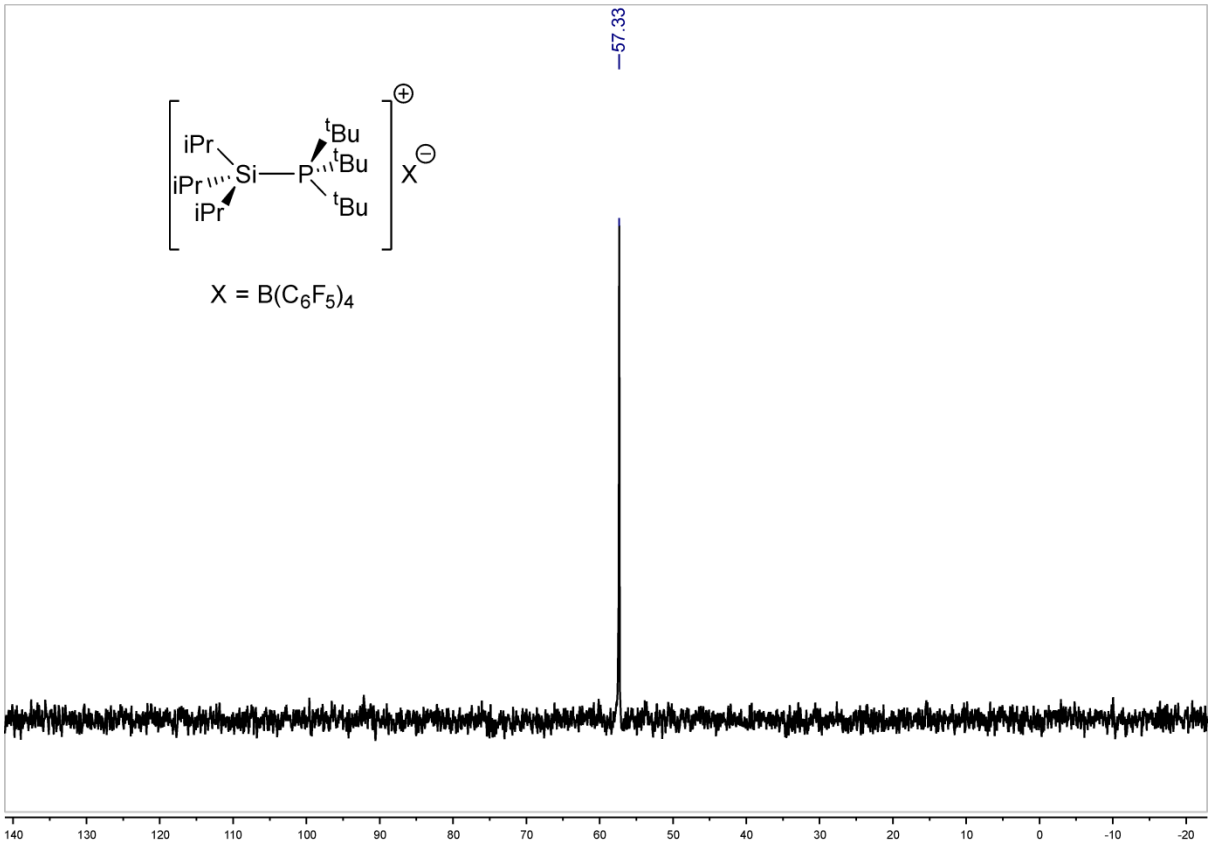

Figure 4. ^{31}P NMR spectrum of **1** in C_6D_5Cl solvent.

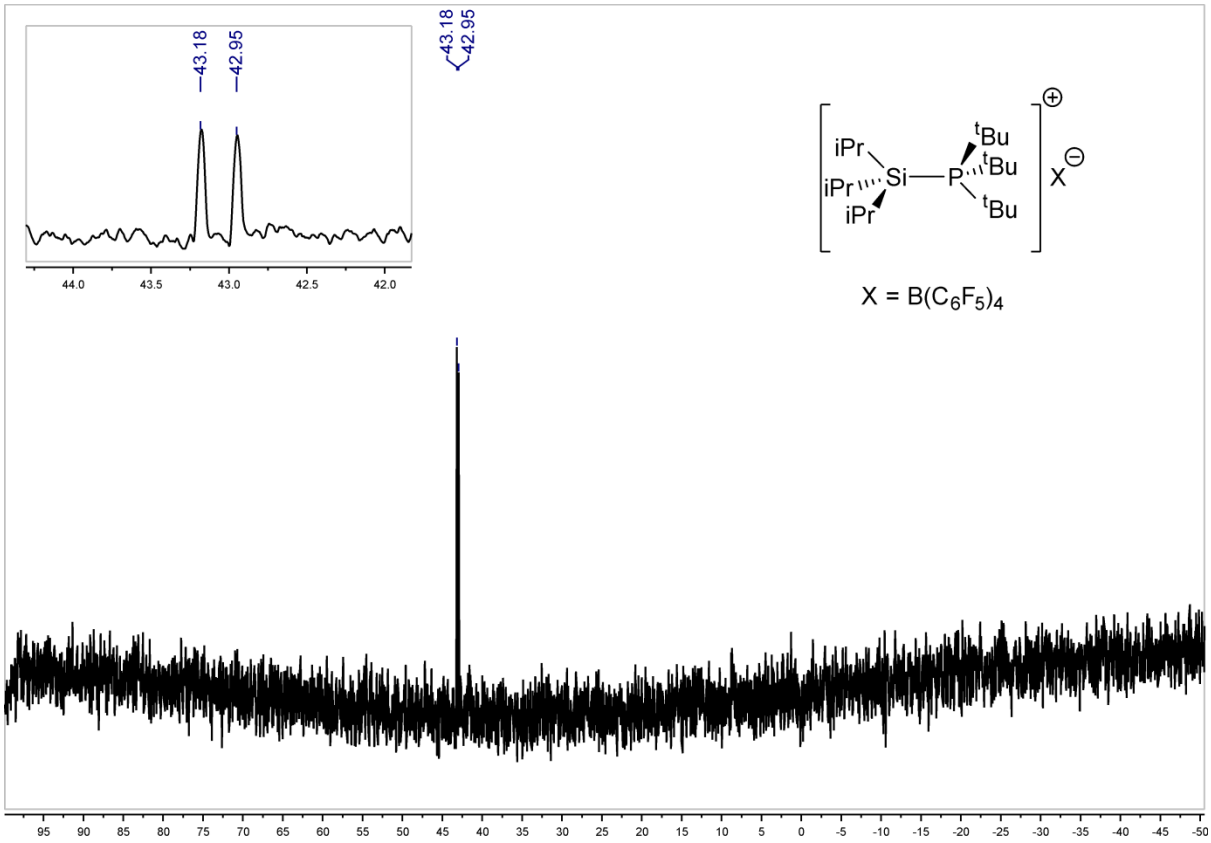

Figure 5. ^{29}Si NMR spectrum of **1** in C_6D_5Cl solvent. Inset reveals expanded region; $^{1}J(Si,P)$ = 23 Hz.

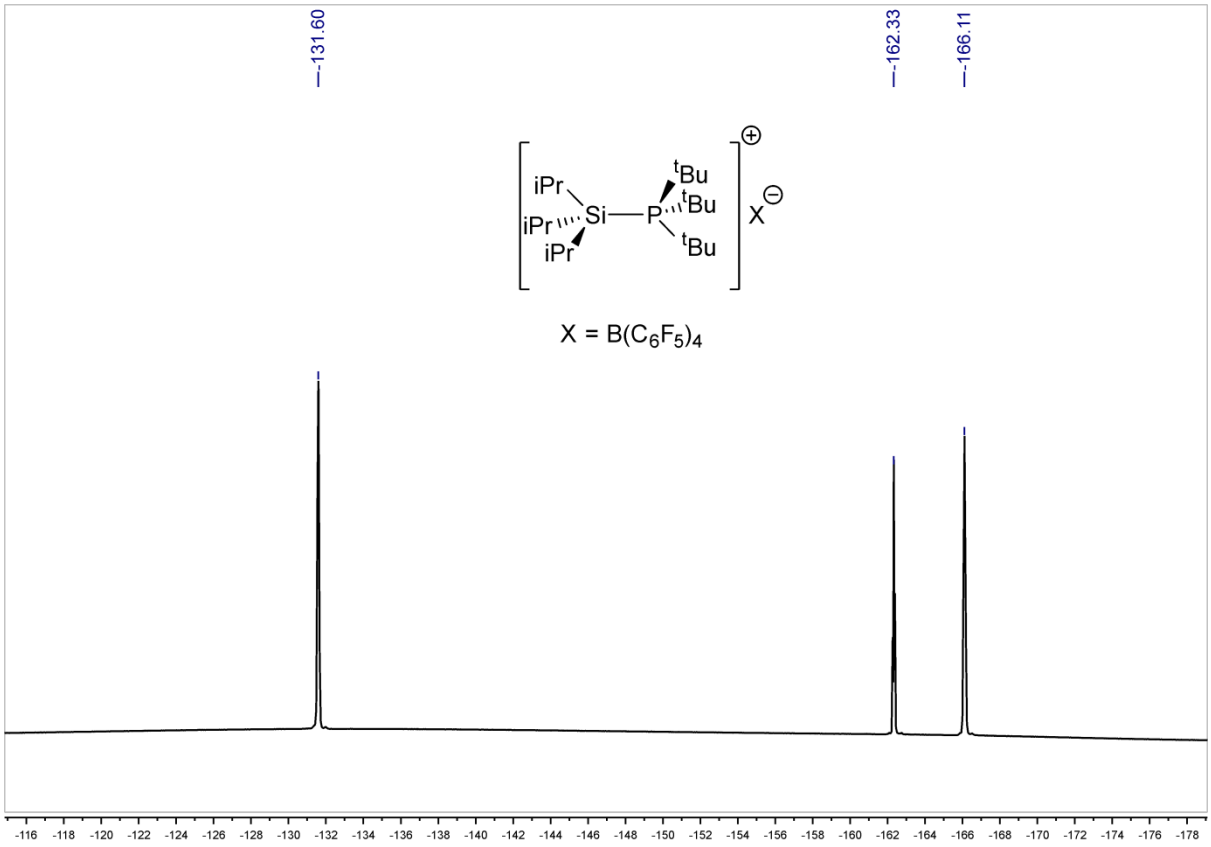

Figure 6. ^{19}F NMR spectrum of **1** in C_6D_5Cl solvent.

S6 High Resolution Mass Spectrometry (ES+) of 1

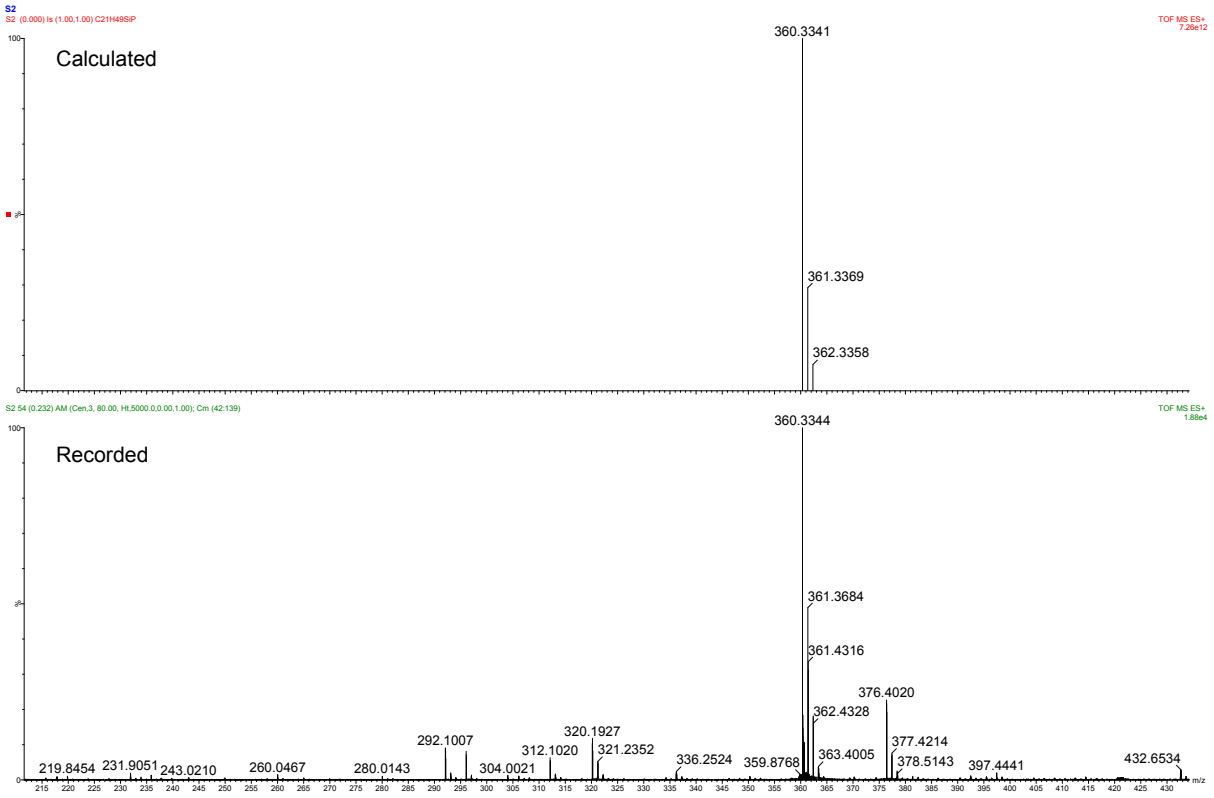

Elemental Composition Report

Single Mass Analysis

Tolerance = 7.0 PPM / DBE: min = -1.5, max = 50.0

Element prediction: Off

Number of isotope peaks used for i-FIT = 3

Monoisotopic Mass, Odd and Even Electron Ions

948 formula(e) evaluated with 2 results within limits (up to 50 best isotopic matches for each mass)

Elements Used:

C: 21-21 H: 0-200 N: 0-10 O: 0-10 Na: 0-1 Si: 0-1 P: 0-1

Minimum:				-1.5			
Maximum:		5.0	7.0	50.0			
Mass	Calc. Mass	mDa	PPM	DBE	i-FIT	i-FIT (Norm)	Formula
360.3344	360.3341	0.3	0.8	-1.0	493.1	0.3	C21 H49 Si P

S7 Variable Temperature ^{31}P NMR spectroscopy of 1

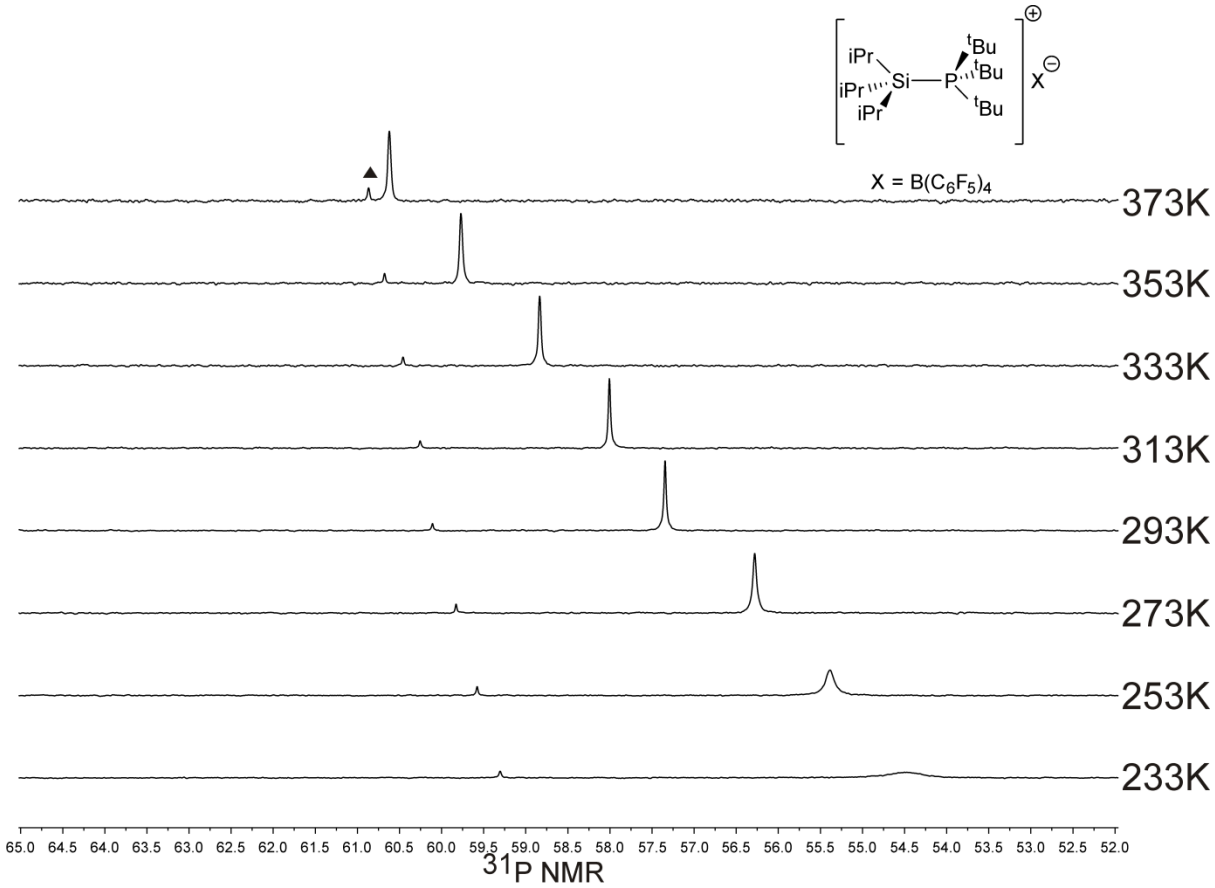

Figure 7. Variable temperature ^{31}P NMR spectroscopy of **1** in C_6D_5Cl solvent. ▲ denotes trace [*t*Bu$_3$PH][B(C$_6$F$_5$)$_4$] (due to adventitious H_2O). Resonances referenced to internal capillary (Ph_3P in C_6D_5Cl; δ = – 5.3 ppm).

S8 D_2 Activation Experiments

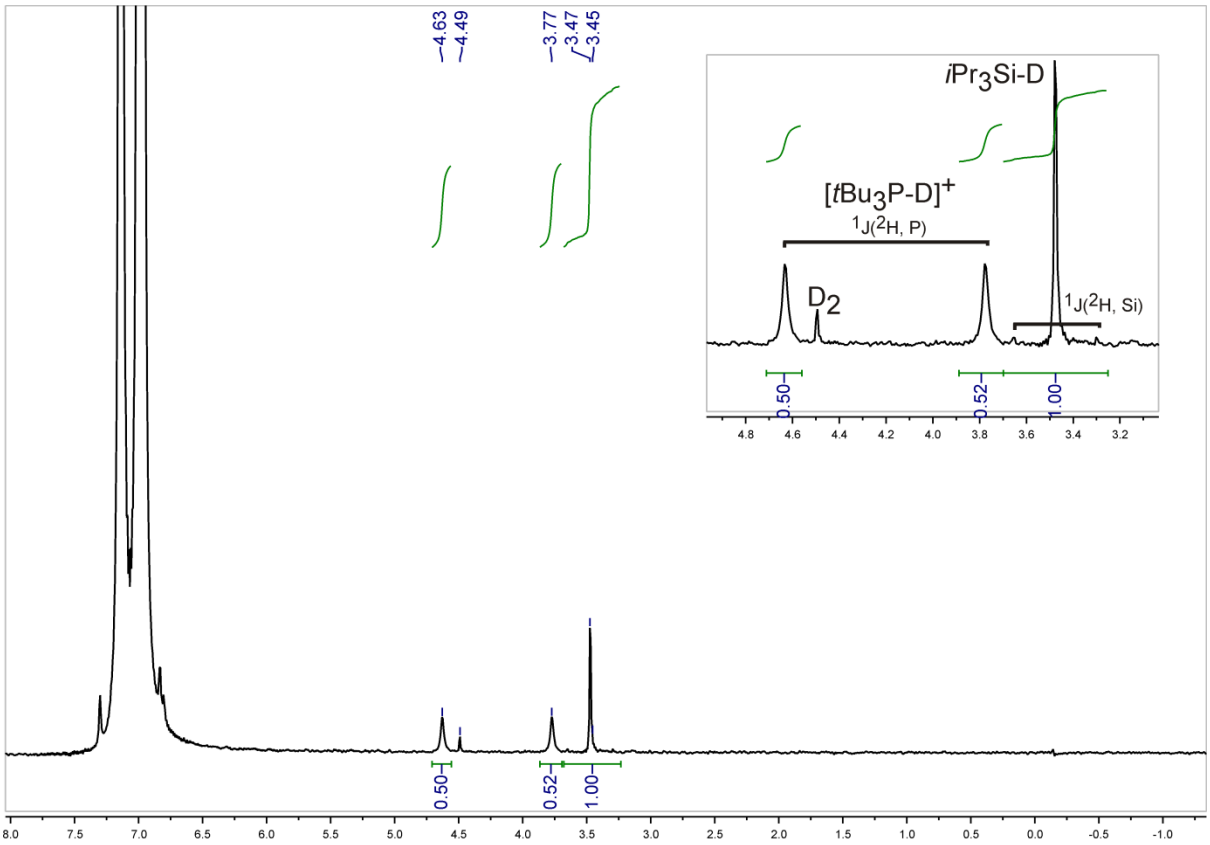

Figure 8. ^{2}H NMR (76.8 MHz) spectrum of [tBu$_3$P-D][B(C$_6$F$_5$)$_4$] and iPr$_3$Si-D products after heating **1** under D_2 atmosphere (4 bar, 90ºC) for 8 hours. $^1J(^2H, P)$ = 66 Hz and $^1J(^2H, ^{29}Si)$ = 27 Hz. Relative integrations of [tBu$_3$P-D]$^+$ and iPr$_3$Si-D resonances show quantitative (1:1) conversion of D_2.

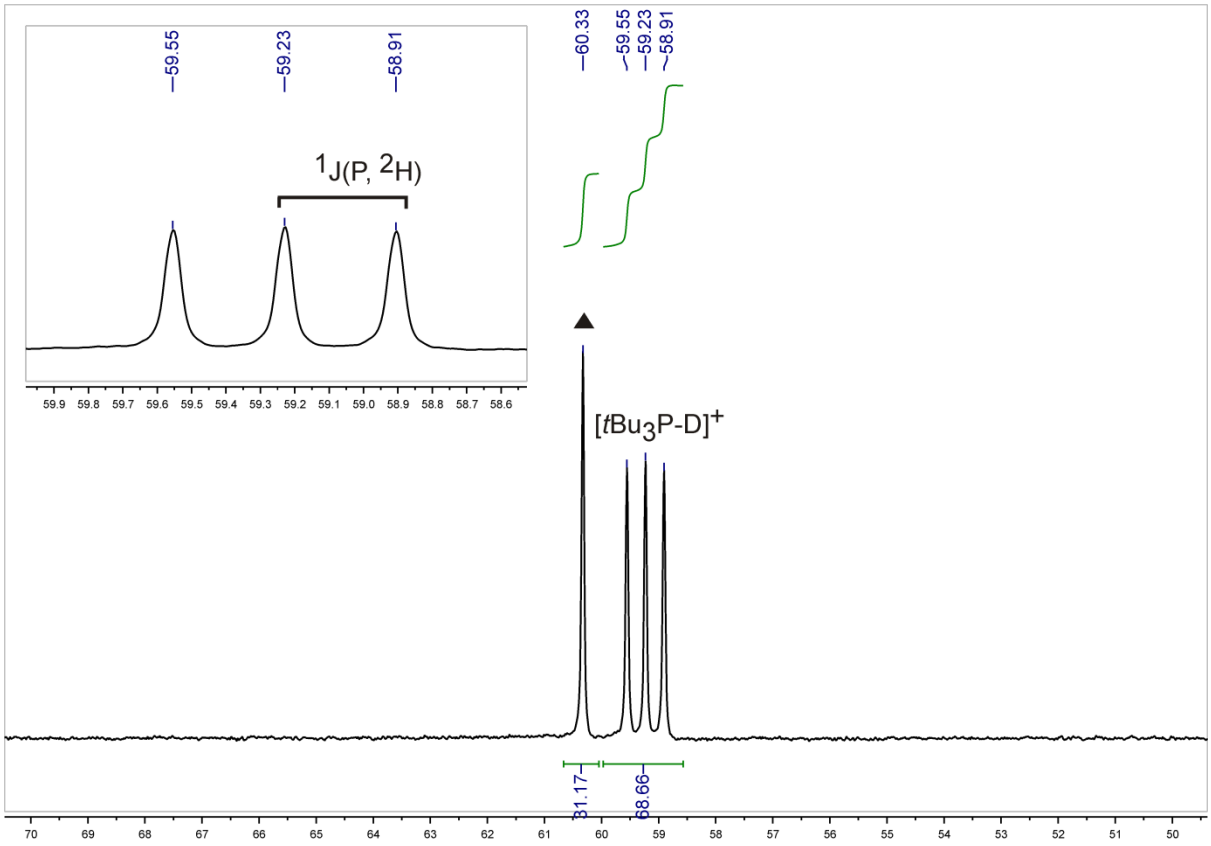

Figure 9. ^{31}P NMR spectrum of $[tBu_3P\text{-}D][B(C_6F_5)_4]$ after heating **1** under D_2 atmosphere (4 bar, 90ºC) for 8 hours. $^1J(^2H, P)$ = 66 Hz. ▲ denotes trace $[tBu_3PH][B(C_6F_5)_4]$ (due to adventitious moisture in D_2).

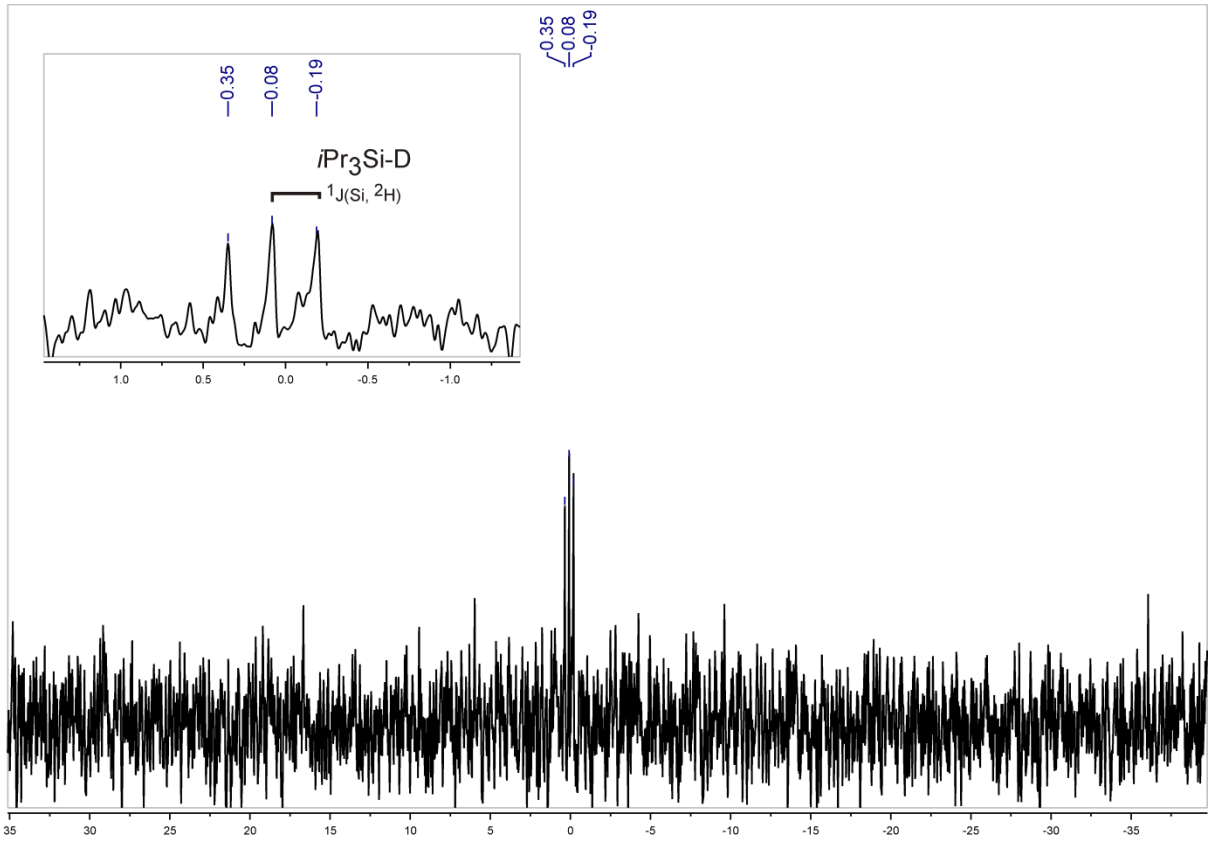

Figure 10. ^{29}Si NMR spectra of $iPr_3Si\text{-}D$ after heating **1** under D_2 atmosphere (4 bar, 90ºC) for 8 hours. $^1J(Si, ^2H)$ = 27 Hz.

S9 ^{31}P and ^{1}H NMR Spectral Data for H_2 Heterolysis Experiments

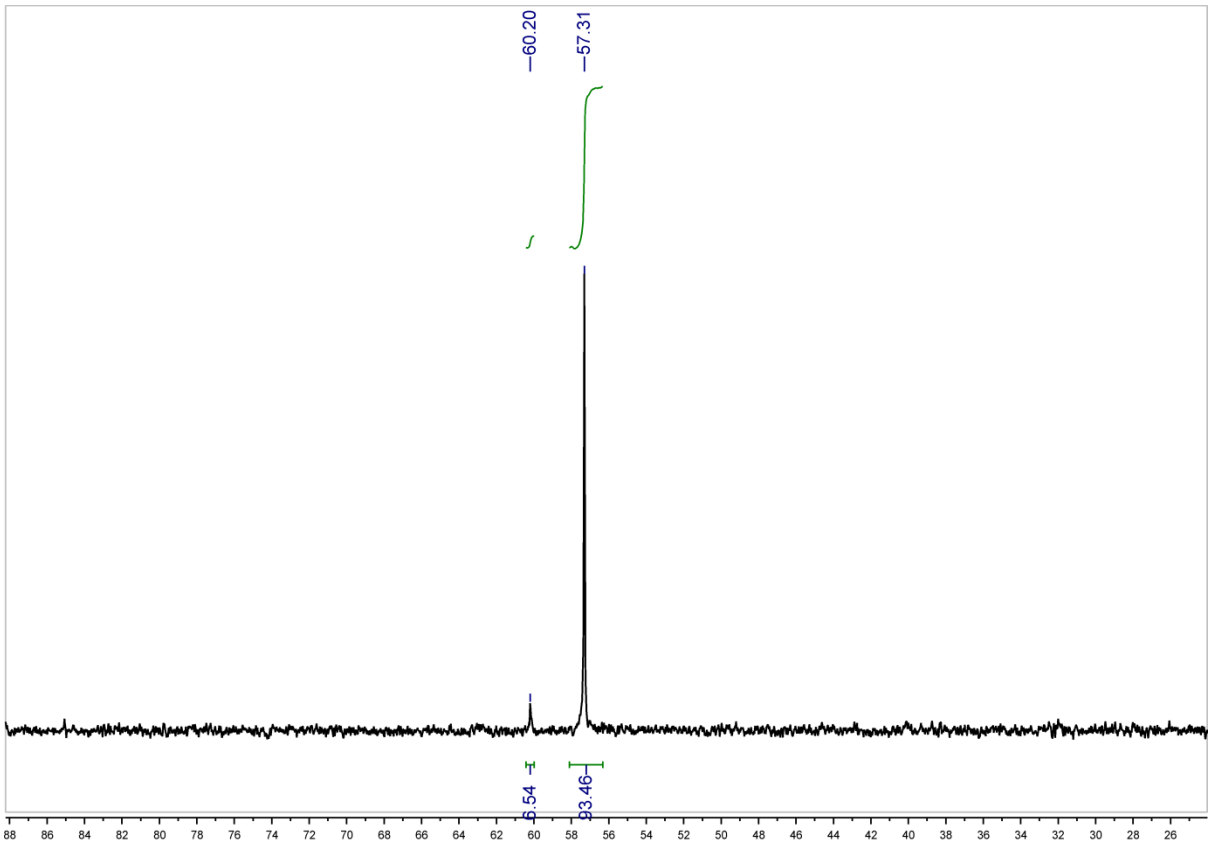

Figure 11. ^{31}P NMR spectrum of **1** under H_2 atmosphere, prior to heating at 90ºC. Presence of [tBu$_3$PH][B(C$_6$F$_5$)$_4$] (δ = 60.2 ppm; *ca.* 6 %) is due to hydrolysis by adventitious moisture in H_2.

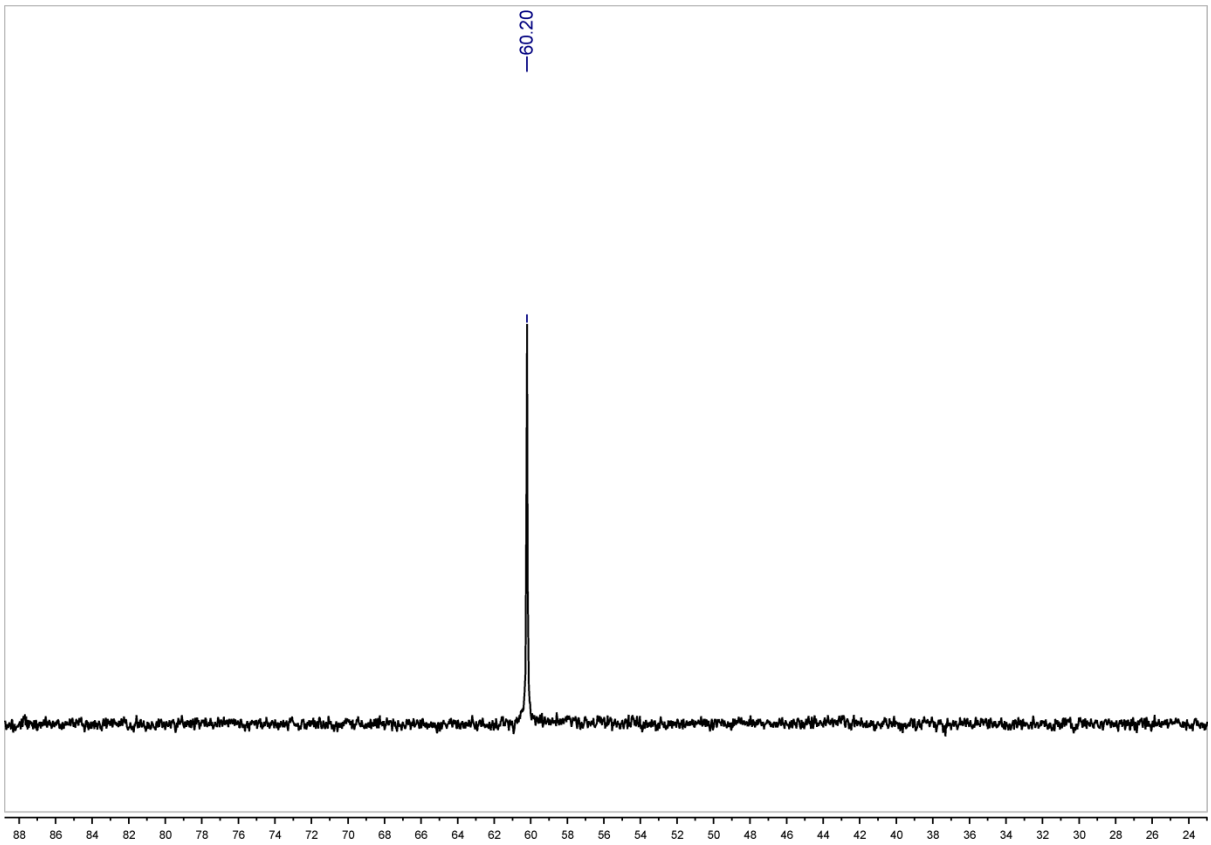

Figure 12. ^{31}P NMR spectrum of [tBu$_3$PH][B(C$_6$F$_5$)$_4$] after H_2 heterolysis by **1** (C$_6$D$_5$Cl, 8 hours, 90ºC).

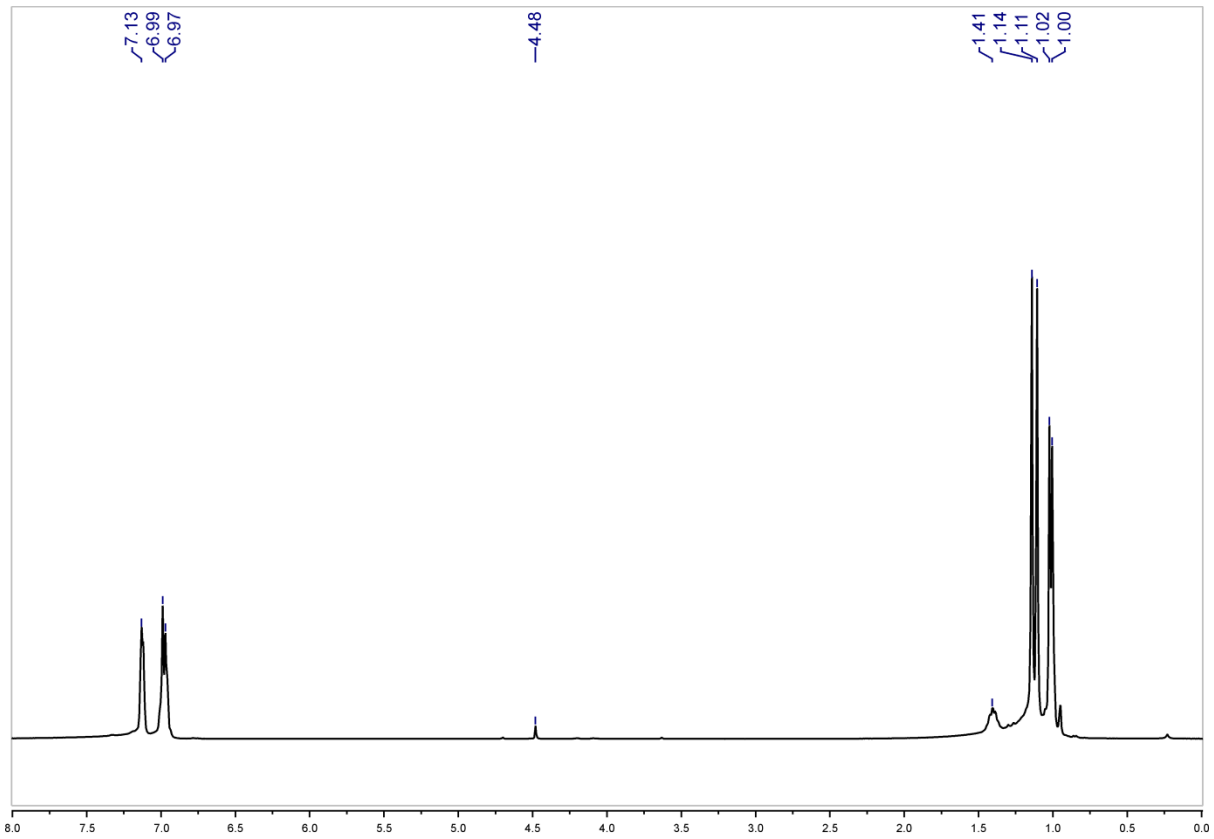

Figure 13. ^{1}H NMR spectrum of **1** under H_2 (C_6D_5Cl, δ = 4.48 ppm) atmosphere, prior to heating at 90ºC.

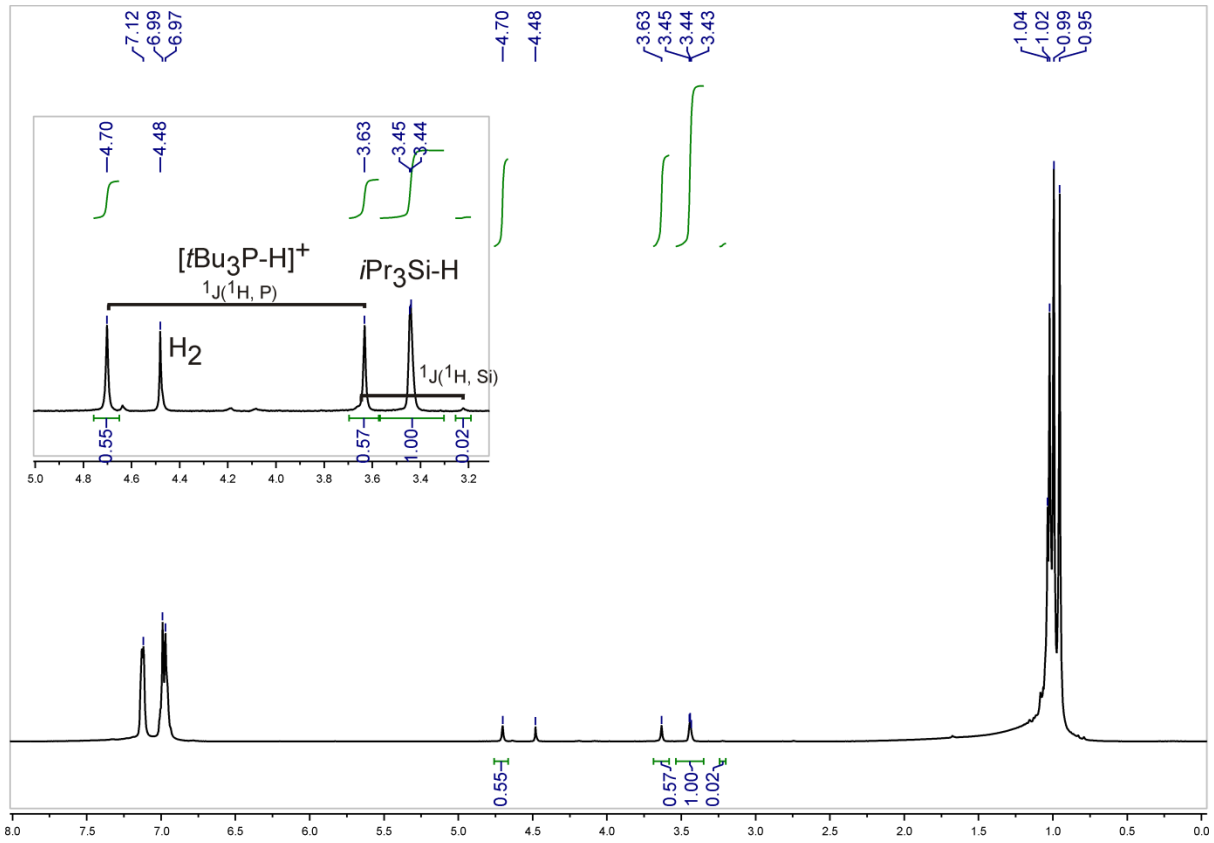

Figure 14. ^{1}H NMR spectrum after heating **1** under H_2 atmosphere (4 bar, 90ºC) for 8 hours; *ca.* 94 % yield iPr$_3$SiH calculated by relative integration of [tBu$_3$P-*H*]$^+$ and iPr$_3$Si-*H* resonances. Remaining 6-7 % ^{31}P deficit attributed to formation of [tBu$_3$P-H]$^+$[B(C$_6$F$_5$)$_4$] and (iPr$_3$Si)$_2$O by initial adventitious hydrolysis (see S4 and main text for explanation), as corroborated by the ^{31}P NMR spectrum in Figure 9.

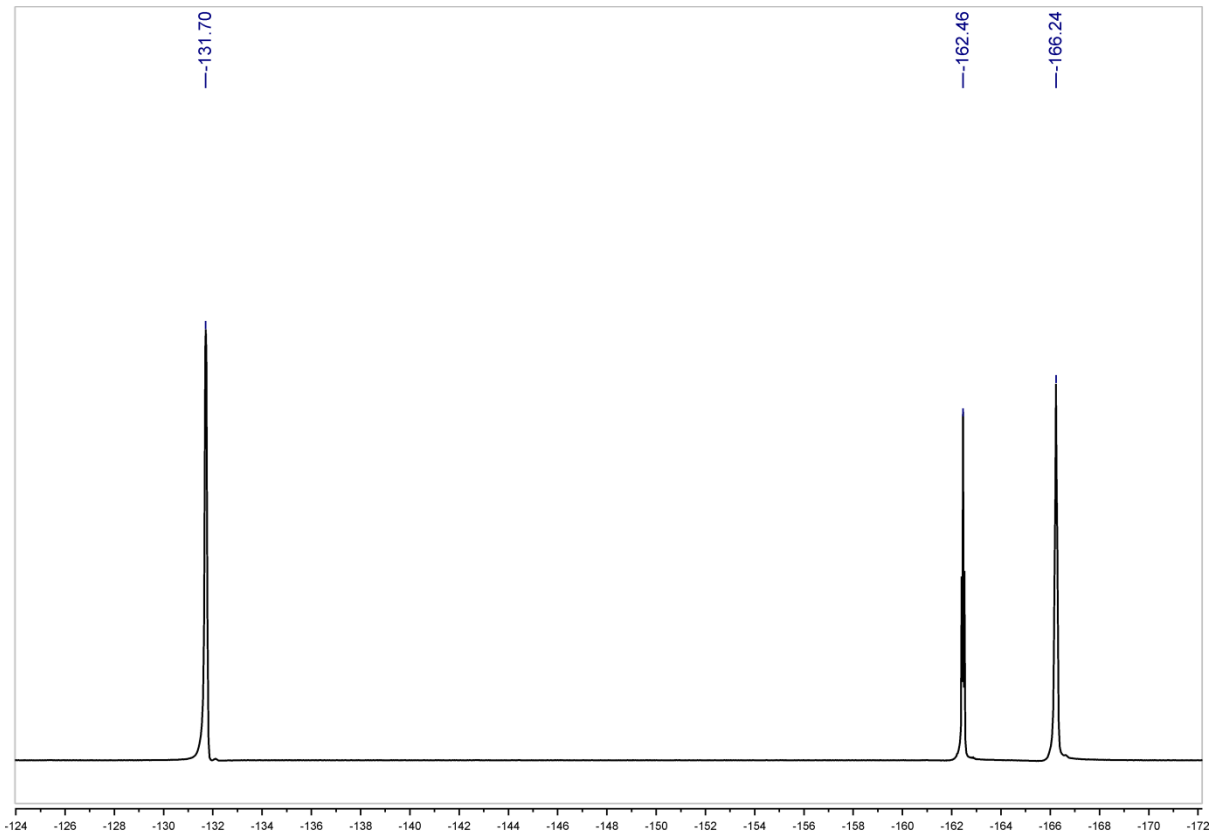

Figure 15. ^{19}F NMR spectrum of **1** ($[B(C_6F_5)_4]^-$ counterion; C_6D_5Cl**),** under H_2 atmosphere.

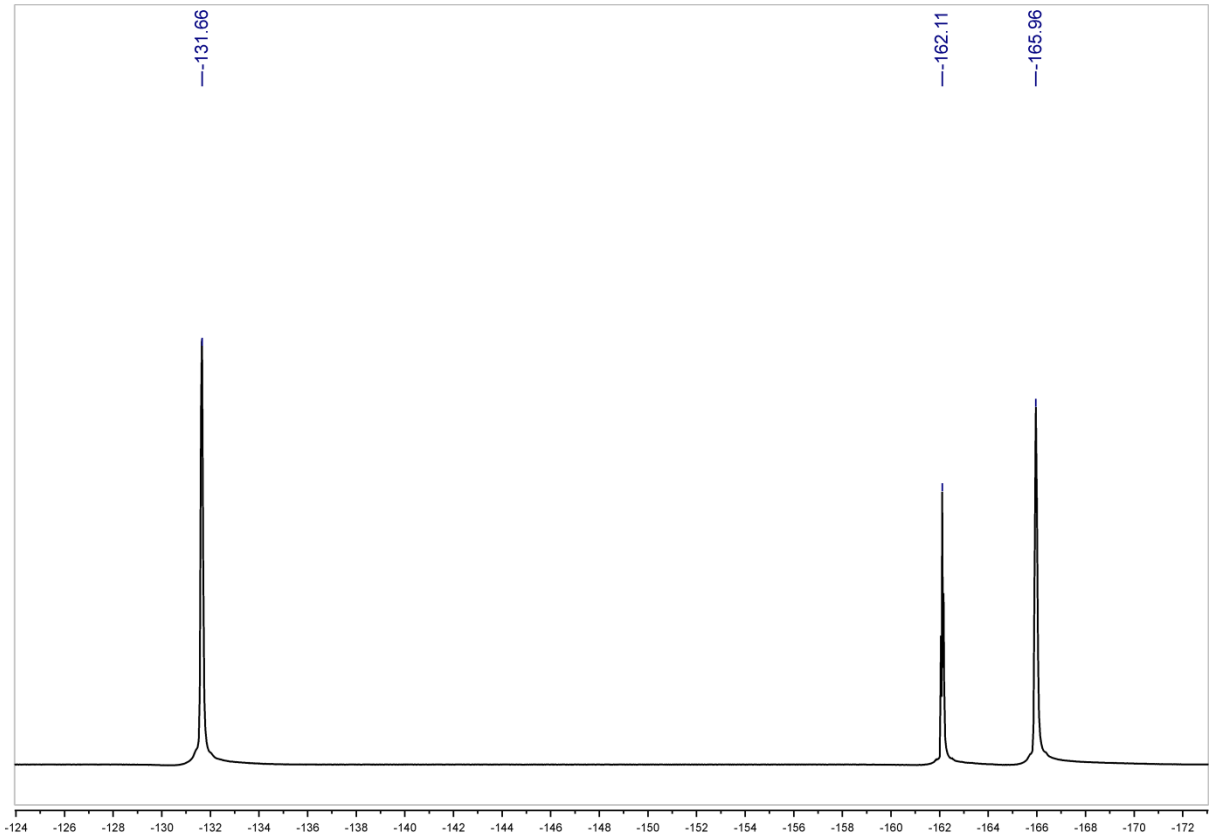

Figure 16. ^{19}F NMR spectrum after heating **1** under H_2 atmosphere (4 bar, 90ºC) for 8 hours, revealing the $[B(C_6F_5)_4]^-$ counterion to be intact after reaction completion.

S10 Synthesis of $[i\text{Pr}_3\text{Si}\cdot\text{ClPh}]^+[\text{B}(\text{C}_6\text{F}_5)_4]^-$ and thermal decomposition experiment

The following is a modified procedure based on that reported by Müller *et al.*[3] Inside a glove-box, $i\text{Pr}_3\text{SiH}$ (0.015 g, 0.095 mmol) and PhCl (0.5 ml) were added to a Teflon® vial and cooled to –25 ºC. After addition of solid $[\text{Ph}_3\text{C}][\text{B}(\text{C}_6\text{F}_5)_4]$ (0.050 g, 0.054 mmol) the mixture was stirred for 5 minutes during which time the solution decolourised. Upon addition of hexanes (0.5 ml), a pale yellow oil formed which was allowed to settle before decanting away the supernatant and rinsing the oil with further hexanes (3 x 0.5 ml). Volatiles were then removed under vacuum leaving a thermally unstable pale yellow oil (which gradually turns brown over several days at room temperature) which was subsequently redissolved in PhCl for subsequent NMR studies; spectral data (^{1}H, ^{19}F, ^{29}Si NMR) matched those previously reported.[3] Upon heating of this solution under H_2 (the tube charged following the procedure detailed in Section S4) to 90°C in the NMR spectrometer (400 MHz) decomposition ensued, as evidenced by the disappearance of the ^{11}B and ^{19}F NMR resonances for the $[\text{B}(\text{C}_6\text{F}_5)_4]$ anion, concomitant with the production of resonances attributable to $\text{B}(\text{C}_6\text{F}_5)_3$[4] and $i\text{Pr}_3\text{SiF}$[5] (see Figures 17 and 18 below).

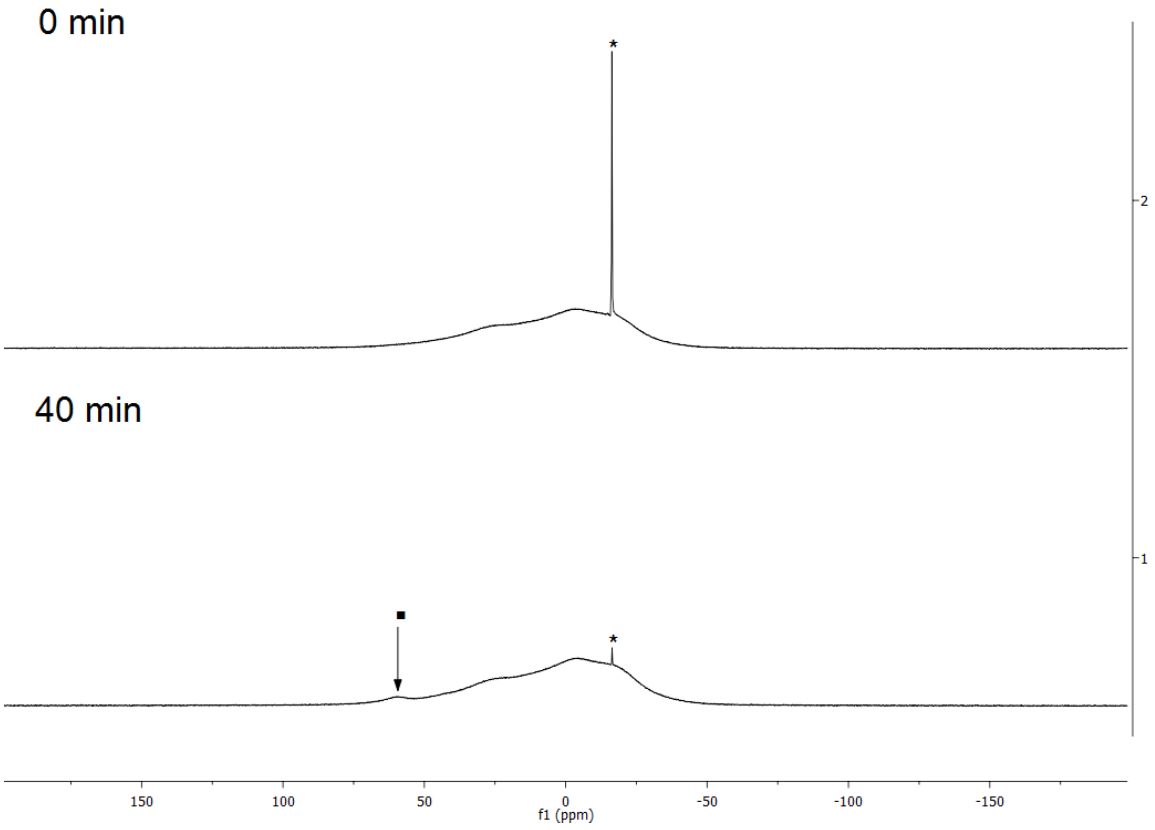

Figure 17. ^{11}B NMR spectrum after heating $[i\text{Pr}_3\text{Si}\cdot\text{ClPh}]^+[\text{B}(\text{C}_6\text{F}_5)_4]^-$ under H_2 atmosphere (4 bar, 90ºC, PhCl solvent) for 40 min, revealing the $[\text{B}(\text{C}_6\text{F}_5)_4]^-$ counterion (resonance denoted *; –16.4 ppm) to decompose into $\text{B}(\text{C}_6\text{F}_5)_3$ (resonance denoted ▪; 59.8 ppm).

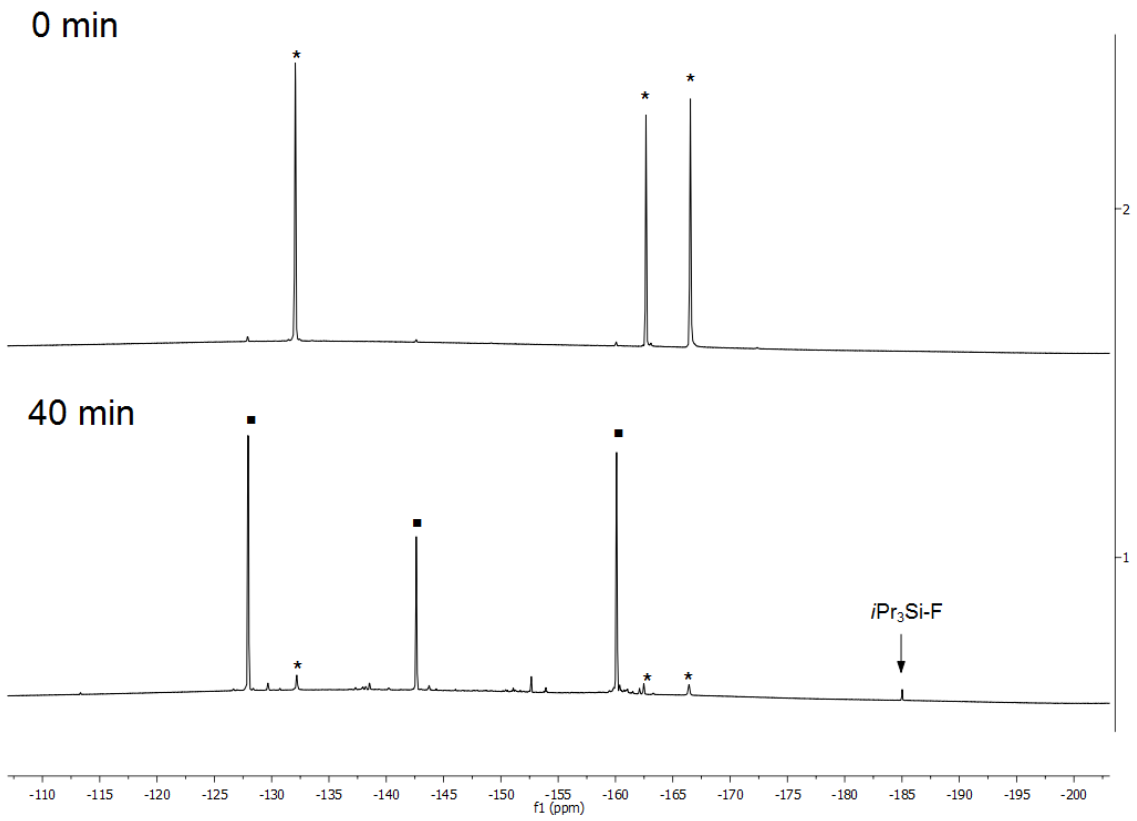

Figure 18. ^{19}F NMR spectrum after heating $[i\text{Pr}_3\text{Si}\cdot\text{ClPh}]^+[\text{B}(\text{C}_6\text{F}_5)_4]^-$ under H_2 atmosphere (4 bar, 90ºC, PhCl solvent) for 40 min, revealing the $[\text{B}(\text{C}_6\text{F}_5)_4]^-$ counterion (resonances denoted *; –132.1, –162.7 and –166.5 ppm) to be decompose into $\text{B}(\text{C}_6\text{F}_5)_3$ (resonances denoted ▪; –128.0, –142.6 and –160.1 ppm) and $i\text{Pr}_3\text{SiF}$ (–160.1 ppm; $^1J_{\text{FSi}}$ = 298 Hz)

S11 Computational Details I

Calculations were performed using Gaussian 09 software suite.[6] Geometry optimisations were initially performed, without symmetry constraints, using the M06-2X density functional in conjunction with the 6-31G(d,p) basis set for all atoms in the gas phase.[7] The M06-2X functional has been shown to produce accurate thermodynamic data in related frustrated Lewis pair systems.[8] Frequency analysis was performed for all stationary points following structure optimisation. This confirmed the nature of the intermediate as either a minimum (no imaginary frequency) or a transition state (only one imaginary frequency). Intrinsic reaction coordinate (IRC) calculations were used to connect transition states and minima located on the potential energy surface allowing a full energy profile of the reaction to be constructed.[9] To better represent the reaction environment and effects of the chlorobenzene solvent, all intermediates were reoptimised and confirmed via vibrational analysis using M06-2X with 6-311+G(d,p) basis set for all atoms and the conductor-like polarisable continuum (C-PCM) model.[10] Energies reported herein are obtained from the solvent-corrected calculations. GaussView 5.0.9 was used to visualise structures, charges and molecular orbitals.[11]

Table S1. Relative energies of H_2 activation intermediates and transition state (363K; kJ mol^{-1}).

Intermediate	ΔE	ΔH	TΔS	ΔG
1 + H_2	0.00	0.00	0.00	0.00
A	0.60	2.00	–19.84	21.85
TS_{AB}	129.80	130.69	–13.69	144.38
B	–61.46	–63.96	–11.93	–52.03
Dissociated products	–44.51	–51.26	39.20	–90.46

Table S2. Various conformers of **1** and their relative enthalpies and Gibbs free energies.

	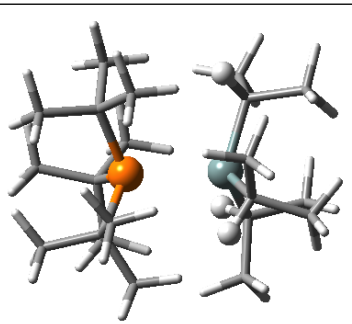	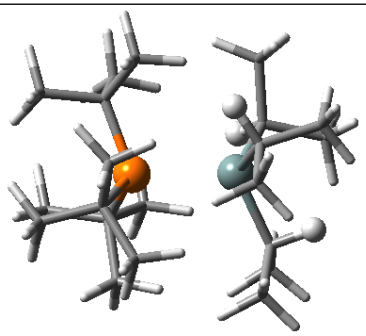	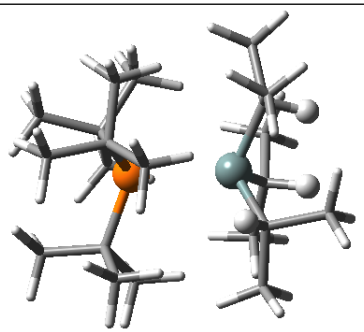	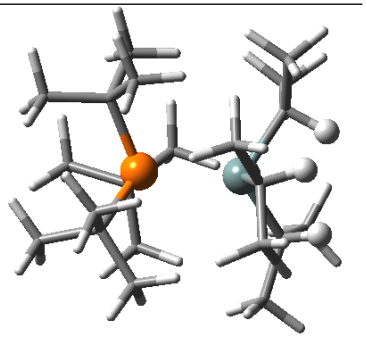
Number of *iso*-propyl methine H atoms pointing towards the P atom	3	2	1	0
ΔH (kJ/mol)	0.00	13.04	19.71	32.17
ΔG (kJ/mol)	0.00	13.29	20.02	31.41

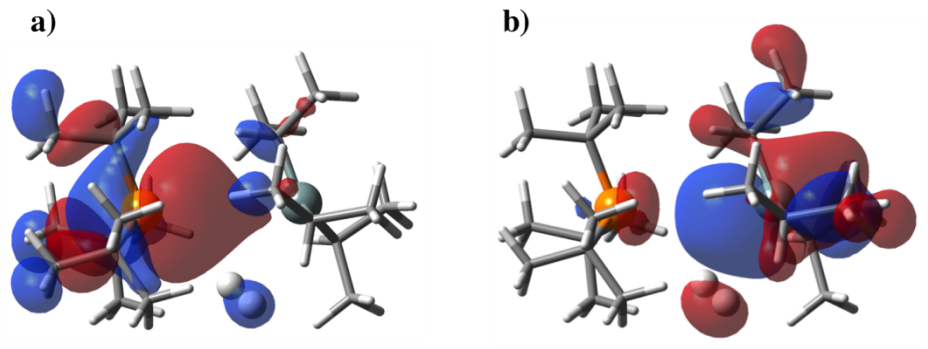

Figure 19. a) HOMO and b) LUMO corresponding to heterolytic H_2 cleavage in TS_{AB}. P atom orange and Si atom grey.

Coordinates of Intermediates

Adduct (1)

```
   71
scf done: -1459.631143
 P    -0.228402     0.025333    -0.003654
Si     2.263574    -0.043970    -0.023136
 C     2.883135     0.400603     1.739471
 H     2.274892    -0.173373     2.444168
 C     2.806763    -1.820357    -0.510955
 C     2.884841     1.238187    -1.310822
 H     2.313835     2.156488    -1.147184
 C     2.730830     0.860068    -2.794857
 H     1.698651     0.865660    -3.134419
 H     3.274322     1.586790    -3.404599
 H     3.141484    -0.125289    -3.022585
 C     4.337184    -0.082012     1.952611
 H     5.044930     0.425758     1.296318
 H     4.627150     0.145248     2.981902
 H     4.457089    -1.154272     1.812442
 C    -0.834982     1.816447    -0.324124
 C    -0.890476    -0.561321     1.698426
 C    -0.930105    -1.120951    -1.372408
 C    -2.417540    -0.867415    -1.675760
 H    -2.588488     0.092979    -2.158301
 H    -2.734718    -1.641269    -2.380938
 H    -3.058678    -0.942091    -0.800478
 C    -0.151448    -0.942196    -2.685396
 H    -0.551759    -1.665675    -3.400888
 H    -0.272598     0.043677    -3.124282
 H     0.911058    -1.152389    -2.576914
 C    -0.771763    -2.594236    -0.961350
 H    -1.437570    -2.882699    -0.151423
 H    -1.038948    -3.203146    -1.828777
 H     0.252756    -2.847633    -0.692715
 C    -2.315754     2.033540     0.034870
 H    -2.577631     3.043638    -0.293516
 H    -2.990359     1.343275    -0.466175
 H    -2.497794     1.990076     1.106969
```

```
 C    -0.646923     2.180471    -1.806436
 H    -0.857381     3.248187    -1.907543
 H     0.372453     2.018663    -2.153445
 H    -1.337237     1.655350    -2.462511
 C    -0.007430     2.824789     0.488636
 H    -0.145582     2.725777     1.561161
 H     1.056468     2.774412     0.264662
 H    -0.349231     3.825384     0.210109
 C    -2.392986    -0.894206     1.685481
 H    -2.680475    -1.106551     2.719335
 H    -3.016588    -0.074567     1.336174
 H    -2.620339    -1.784562     1.102576
 C    -0.653673     0.523793     2.762231
 H    -1.291084     1.394698     2.628739
 H    -0.905983     0.087131     3.731949
 H     0.386210     0.843101     2.813942
 C    -0.140429    -1.816461     2.172235
 H     0.933029    -1.658539     2.259356
 H    -0.512998    -2.059105     3.171197
 H    -0.318394    -2.684284     1.544126
 H     2.196576    -2.113722    -1.369848
 C     4.269602    -1.835521    -1.013619
 H     4.981174    -1.559184    -0.234691
 H     4.513122    -2.853209    -1.330243
 H     4.435698    -1.183153    -1.868314
 C     2.793795     1.880035     2.155362
 H     1.775115     2.218101     2.325203
 H     3.339010     2.018520     3.092870
 H     3.239871     2.551562     1.419529
 C     4.362758     1.612909    -1.049795
 H     4.530782     2.026422    -0.057474
 H     5.037165     0.765915    -1.181168
 H     4.656276     2.377572    -1.773917
 C     2.646902    -2.913444     0.560780
 H     3.151279    -3.821595     0.219947
 H     3.094491    -2.634012     1.516333
 H     1.610520    -3.176625     0.754297
```

Adduct + H_2 (A)

```
   73
scf done: -1460.800559
 P     0.758988    -0.605859     0.000000
Si     3.151346    -0.497878    -0.703199
 C     4.205800    -0.061053     0.840682
 C     3.642265    -2.215983    -1.405742
 C     3.311910     0.863529    -2.047188
 H     2.753253     1.732373    -1.687743
 C     4.778487     1.335277    -2.182530
 H     5.439333     0.544021    -2.538829
 H     4.813464     2.143460    -2.917928
 H     5.190508     1.725381    -1.254111
 H     3.853478    -0.695136     1.659136
 C     4.143564     1.396895     1.329480
 H     3.197005     1.650285     1.800011
 H     4.926150     1.556749     2.076167
 H     4.311271     2.117940     0.526786
 C    -0.022988     1.144943    -0.047802
```

C	0.631195	-1.294659	1.785927
C	-0.221686	-1.757275	-1.180342
C	-1.747216	-1.602784	-1.055758
H	-2.103309	-0.643589	-1.426870
H	-2.197814	-2.376310	-1.684426
H	-2.118076	-1.749218	-0.043990
C	0.155167	-1.484688	-2.645152
H	-0.379685	-2.214200	-3.259400
H	-0.142305	-0.497911	-2.987709
H	1.217885	-1.619015	-2.838955
C	0.133303	-3.226898	-0.900122
H	-0.265525	-3.587559	0.045217
H	-0.323209	-3.827757	-1.690850
H	1.205790	-3.413003	-0.932188
C	-1.359628	1.236315	0.708658
H	-1.763711	2.235446	0.521228
H	-2.101499	0.516822	0.369809
H	-1.238963	1.138692	1.785825
C	-0.270074	1.574869	-1.503396
H	-0.570581	2.625561	-1.484175
H	0.625096	1.507095	-2.120014
H	-1.076612	1.021100	-1.978478
C	0.928472	2.185800	0.563290
H	1.099023	2.041088	1.626288
H	1.890583	2.228255	0.055289
H	0.458316	3.165686	0.443681
C	-0.789770	-1.742880	2.169071
H	-0.762992	-2.012462	3.228944
H	-1.538956	-0.963331	2.051006
H	-1.111904	-2.627924	1.623932
C	1.081589	-0.227780	2.797231
H	0.376043	0.594628	2.888964
H	1.138521	-0.711594	3.775620
H	2.070813	0.170166	2.576257
C	1.565299	-2.500807	1.972062
H	2.606383	-2.263961	1.760376
H	1.508438	-2.797115	3.023026
H	1.274488	-3.363419	1.379795
H	2.835248	-2.529521	-2.074020
C	4.903630	-2.106067	-2.293785
H	5.784652	-1.799079	-1.728734
H	5.115083	-3.092660	-2.714644
H	4.781937	-1.418273	-3.128062
H	2.630028	4.836198	1.938183
H	3.070589	4.306038	1.665480
C	2.777401	0.520810	-3.448860
H	1.692842	0.470914	-3.494042
H	3.093347	1.298219	-4.149659
H	3.161770	-0.428969	-3.825584
C	3.860563	-3.347412	-0.385596
H	4.312951	-4.202478	-0.895016
H	4.534577	-3.060366	0.423733
H	2.938751	-3.698229	0.070680
C	5.687766	-0.444691	0.621281
H	6.239720	-0.225072	1.539039
H	5.828302	-1.501672	0.404680
H	6.152105	0.129142	-0.181687

H_2 Activation Transition State (TS_{AB})

```
   73
scf done: -1460.747048
 P     0.024186     0.176631    -0.006777
Si     4.077924     0.336243    -0.569220
 C     5.304406     0.350691     0.823013
 C     3.579998    -1.316804    -1.254263
 C     3.860368     1.853955    -1.617059
 H     3.681642     2.685742    -0.927988
 C     5.198342     2.126489    -2.349275
 H     5.484578     1.301039    -3.006173
 H     5.070172     3.012740    -2.975070
 H     6.022399     2.324656    -1.661606
 H     4.966703    -0.362835     1.581681
 C     5.614120     1.704917     1.467744
 H     4.809463     2.046668     2.117208
 H     6.512682     1.611013     2.081947
 H     5.807557     2.479551     0.721182
 C    -1.045602     1.754828    -0.232326
 C    -0.218008    -0.414643     1.805912
 C    -0.710059    -1.172791    -1.156291
 C    -2.240392    -1.297040    -1.191492
 H    -2.717460    -0.418725    -1.624787
 H    -2.504443    -2.152067    -1.823802
 H    -2.671492    -1.469437    -0.206355
 C    -0.215073    -0.901935    -2.592151
 H    -0.536603    -1.732115    -3.229223
 H    -0.615732     0.011900    -3.022963
 H     0.874426    -0.849184    -2.647746
 C    -0.126531    -2.542084    -0.765655
 H    -0.535158    -2.926574     0.167593
 H    -0.381239    -3.259797    -1.551551
 H     0.962948    -2.518607    -0.682673
 C    -2.427136     1.745646     0.438082
 H    -2.944446     2.675715     0.177695
 H    -3.046504     0.917136     0.093970
 H    -2.373062     1.702020     1.524231
 C    -1.263400     2.057256    -1.725527
 H    -1.688643     3.062863    -1.803242
 H    -0.331064     2.054992    -2.293191
 H    -1.965978     1.374138    -2.199741
 C    -0.218271     2.940054     0.302749
 H     0.031523     2.859480     1.358562
 H     0.712046     3.048187    -0.262423
 H    -0.797149     3.859743     0.169269
 C    -1.545945    -1.111332     2.135877
 H    -1.565341    -1.330091     3.209152
 H    -2.411037    -0.487826     1.910971
 H    -1.661659    -2.060286     1.613847
 C    -0.045643     0.762436     2.783643
 H    -0.860567     1.481991     2.745318
 H    -0.024168     0.351987     3.798133
 H     0.896224     1.290666     2.629370
 C     0.942605    -1.373790     2.131889
 H     1.905992    -0.867832     2.015743
 H     0.858078    -1.684719     3.178301
 H     0.947510    -2.274313     1.521643
```

H	2.526430	-1.192369	-1.522614
C	4.373231	-1.586005	-2.555987
H	5.442212	-1.704175	-2.364339
H	4.011201	-2.521035	-2.989969
H	4.242382	-0.802706	-3.304547
H	2.897769	2.123970	1.341119
H	2.324379	1.767792	1.026170
C	2.691290	1.748784	-2.603516
H	1.757200	1.516559	-2.090390
H	2.572309	2.698729	-3.129899
H	2.868798	0.975099	-3.354704
C	3.716396	-2.481123	-0.266175
H	3.352071	-3.397787	-0.737084
H	4.758090	-2.651071	0.014902
H	3.140783	-2.320008	0.645990
C	6.582856	-0.240044	0.157027
H	7.350736	-0.335209	0.927628
H	6.429779	-1.231205	-0.273257
H	6.981038	0.417528	-0.620007

H_2 Activation Products (B)

73

P	-0.215736	0.368020	0.000000
Si	4.281765	1.267341	-0.653804
C	5.623635	0.684490	0.548724
C	3.681672	-0.107919	-1.817714
C	4.728917	2.859699	-1.577505
H	4.727290	3.646138	-0.811703
C	6.116348	2.853631	-2.235859
H	6.223416	2.033986	-2.951741
H	6.281077	3.788270	-2.781577
H	6.916826	2.757641	-1.499526
H	5.123589	-0.040857	1.204497
C	6.089099	1.860119	1.421372
H	5.251680	2.358082	1.918347
H	6.781802	1.516929	2.195769
H	6.613354	2.611306	0.822942
C	-0.923694	1.996932	-0.601610
C	-0.197895	0.177589	1.865393
C	-0.846155	-1.141210	-0.923960
C	-2.379562	-1.136270	-1.002685
H	-2.765146	-0.312607	-1.602738
H	-2.691641	-2.065873	-1.485306
H	-2.847665	-1.101950	-0.017260
C	-0.227011	-1.157938	-2.335088
H	-0.518998	-2.100700	-2.804613
H	-0.571966	-0.353665	-2.977232
H	0.864686	-1.135962	-2.293601
C	-0.376615	-2.433739	-0.234220
H	-0.797925	-2.574441	0.758691
H	-0.721534	-3.264898	-0.854109
H	0.711703	-2.497360	-0.181547
C	-2.319955	2.255458	-0.018425
H	-2.684661	3.198012	-0.435222
H	-3.036358	1.477004	-0.283940
H	-2.306035	2.362913	1.065988

```
 C    -1.001063     1.985623    -2.137274
 H    -1.313105     2.984574    -2.450523
 H    -0.030237     1.783222    -2.596134
 H    -1.738376     1.282604    -2.519928
 C     0.040936     3.134721    -0.209004
 H    -0.015834     3.400080     0.842104
 H     1.078511     2.899430    -0.456543
 H    -0.245642     4.017940    -0.784836
 C    -1.548117    -0.342087     2.381033
 H    -1.498497    -0.370058     3.472563
 H    -2.375367     0.315266     2.106216
 H    -1.776046    -1.350299     2.038574
 C     0.106945     1.524827     2.541104
 H    -0.703861     2.243664     2.437357
 H     0.227376     1.323172     3.608384
 H     1.037940     1.967526     2.182327
 C     0.951815    -0.773129     2.249612
 H     1.917716    -0.372924     1.929700
 H     0.968603    -0.838247     3.340525
 H     0.840634    -1.782754     1.865084
 H     2.723454     0.254607    -2.218907
 C     4.598693    -0.393155    -3.015923
 H     5.601948    -0.684377    -2.693794
 H     4.196129    -1.214809    -3.617213
 H     4.699385     0.475298    -3.669432
 H     3.096312     1.603831     0.204412
 H     1.142898     0.445894    -0.352193
 C     3.641517     3.205858    -2.606364
 H     2.644039     3.238186    -2.158660
 H     3.833706     4.183953    -3.057777
 H     3.615382     2.471382    -3.416822
 C     3.421537    -1.397926    -1.025537
 H     2.959980    -2.165225    -1.656543
 H     4.357595    -1.814614    -0.642432
 H     2.770935    -1.235519    -0.159392
 C     6.821779    -0.022474    -0.101023
 H     7.560605    -0.293075     0.660163
 H     6.527650    -0.940960    -0.613549
 H     7.324375     0.617978    -0.830581
```

H_2

```
    2
scf done:    -1.168538
 H    -0.762397     0.062069     0.000000
 H    -1.506569     0.062069     0.000000
```

***i*Pr_3SiH**

```
   32
scf done:  -645.613642
Si     0.269235     0.304480    -0.003971
 C     2.066426     0.711594     0.447714
 C    -0.007523    -1.546716    -0.314425
 H     0.131238    -2.024243     0.664363
 C    -0.399417     1.391322    -1.408110
 H    -1.490383     1.277262    -1.361628
 C     0.049441     0.988511    -2.819876
```

H	-0.303965	-0.008541	-3.091374
H	-0.346886	1.691208	-3.560525
H	1.138579	0.991657	-2.917011
H	2.029016	1.716063	0.889251
C	3.044694	0.760128	-0.734346
H	2.784784	1.545184	-1.447605
H	4.061166	0.961027	-0.379588
H	3.070581	-0.187322	-1.279522
C	0.977213	-2.200704	-1.293855
H	2.004291	-2.164918	-0.924389
H	0.719082	-3.253886	-1.447461
H	0.960384	-1.714243	-2.273002
H	-0.545310	0.645377	1.203062
C	2.568052	-0.255395	1.530824
H	3.561429	0.038298	1.884504
H	1.899558	-0.282790	2.396026
H	2.647289	-1.275233	1.141792
C	-0.072829	2.866753	-1.131928
H	-0.552442	3.516281	-1.871011
H	-0.410796	3.181733	-0.140585
H	1.004962	3.048375	-1.186891
C	-1.458758	-1.795213	-0.752536
H	-1.665906	-2.867816	-0.821564
H	-2.177443	-1.360174	-0.052219
H	-1.652533	-1.360364	-1.737945

[*t*Bu$_3$PH]$^+$

41

scf done: -815.204240

P	0.261626	1.053730	0.000446
C	0.366226	2.869891	0.459490
C	1.780776	0.053508	0.462924
C	-1.364496	0.237397	0.459167
C	-1.721402	0.499056	1.929723
H	-1.919001	1.550814	2.133495
H	-2.636659	-0.054773	2.153902
H	-0.947919	0.149434	2.615516
C	-2.472466	0.766579	-0.472288
H	-3.368994	0.173090	-0.276778
H	-2.728199	1.807071	-0.299251
H	-2.212494	0.634715	-1.524957
C	-1.279521	-1.279481	0.220378
H	-0.598247	-1.781944	0.904086
H	-2.277393	-1.686161	0.400639
H	-1.007724	-1.519298	-0.809376
C	0.768916	3.048227	1.930568
H	0.748451	4.117972	2.154048
H	0.077119	2.554681	2.615156
H	1.777539	2.691803	2.136485
C	-0.989658	3.554562	0.218800
H	-0.843130	4.622230	0.398571
H	-1.332413	3.438601	-0.811133
H	-1.766297	3.216321	0.901859
C	1.380062	3.564418	-0.470397
H	2.408399	3.262670	-0.298322
H	1.135417	3.408294	-1.523401
H	1.317282	4.637212	-0.272192

C	1.729328	-0.386340	1.933295
H	2.663439	-0.907766	2.157366
H	1.650918	0.459019	2.618919
H	0.912989	-1.078228	2.137163
C	3.053641	0.884119	0.228289
H	3.144603	1.727439	0.909862
H	3.903150	0.223162	0.416021
H	3.132329	1.235846	-0.802162
C	1.877117	-1.170275	-0.468918
H	1.865719	-0.878346	-1.521447
H	2.837589	-1.652156	-0.270367
H	1.101637	-1.910501	-0.299320
H	0.263929	1.052425	-1.403798

S12 Computational Details II (QTAIM analysis)

Bader's Atoms in Molecules (QTAIM) theory provides a means of analyzing the topology of the electron density (p(r)) to describe interatomic interactions and rationalise chemical bonding. Electron properties including bond critical points (BCP), the Laplacian of the electron density ($\nabla^2\rho(r)$) and the local electron kinetic (G), potential (V) and total (H) energy densities can be derived using QTAIM to reveal the nature of these interactions. The presence of a BCP indicates the lowest point of electron density between two nuclei and the bond path represents the line of maximum electron density. Should the Laplacian of the electron density at a BCP indicate a large and negative value this signifies the electronic charge is concentrated locally between the two nuclei. This is typical of a covalent or 'shared' interaction. Conversely, a small and positive value for the Laplacian indicates depletion of charge along the bond path. This is representative of an interaction between closed shell systems such as ionic bonding, van der Waals interactions and hydrogen bonding.

We have used QTAIM to examine the types of interactions between the fragments that comprise the H_2 activation transition state (**TS_{AB}**) in an attempt to rationalise the stabilising interactions at long Si···P distances (greater than the sum of the van der Waal radii).

Table S3. Selected ρ(r) and $\nabla^2\rho(r)$ values (in a.u.) corresponding to C–H···P, P···H and Si···H interactions.

Viewing Orientation	Side On
ρ(r)	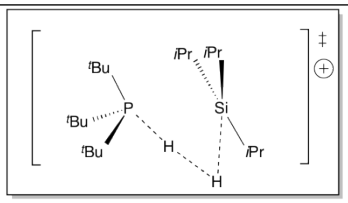 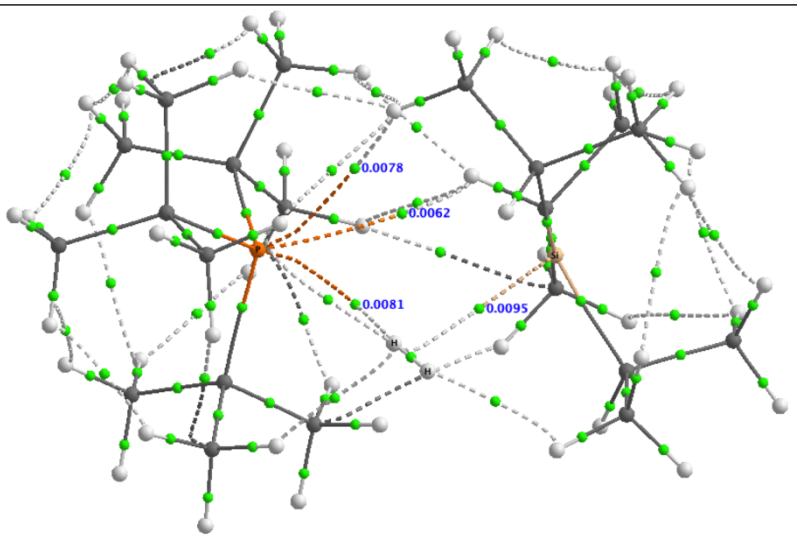
$\nabla^2\rho(r)$	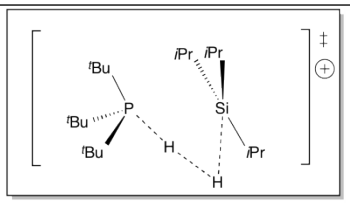 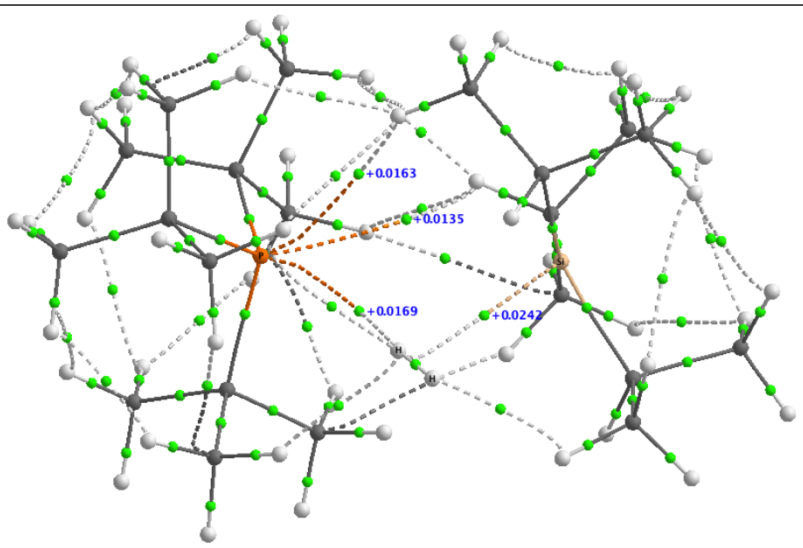

Table S4. Selected ρ(r) and $\nabla^2\rho(r)$ values (in a.u.) corresponding to C–H···H–C and C–H···C interactions.

Viewing Orientation	Top Down
ρ(r)	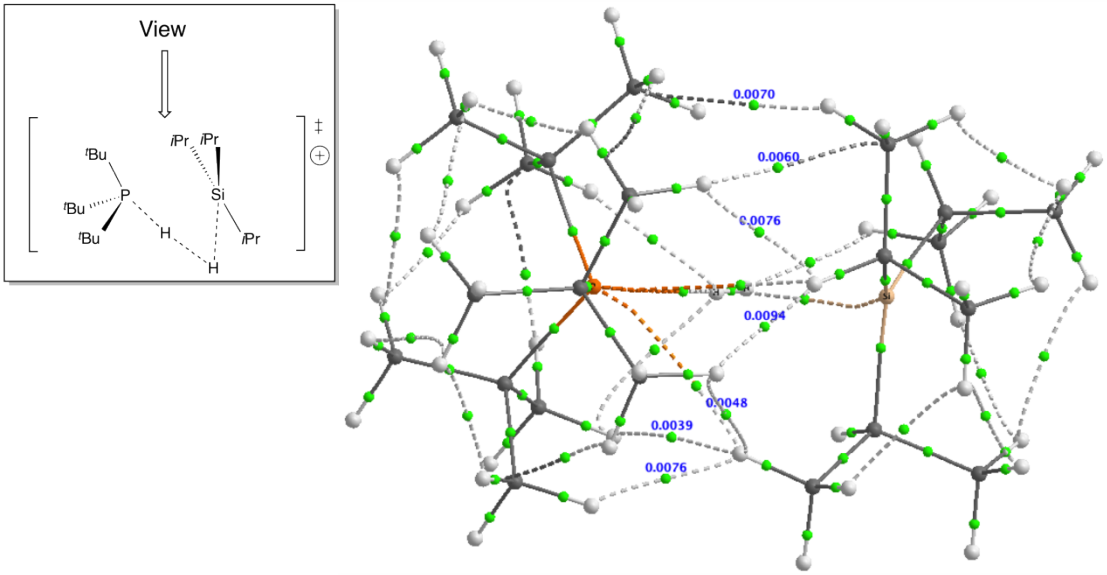
$\nabla^2\rho(r)$	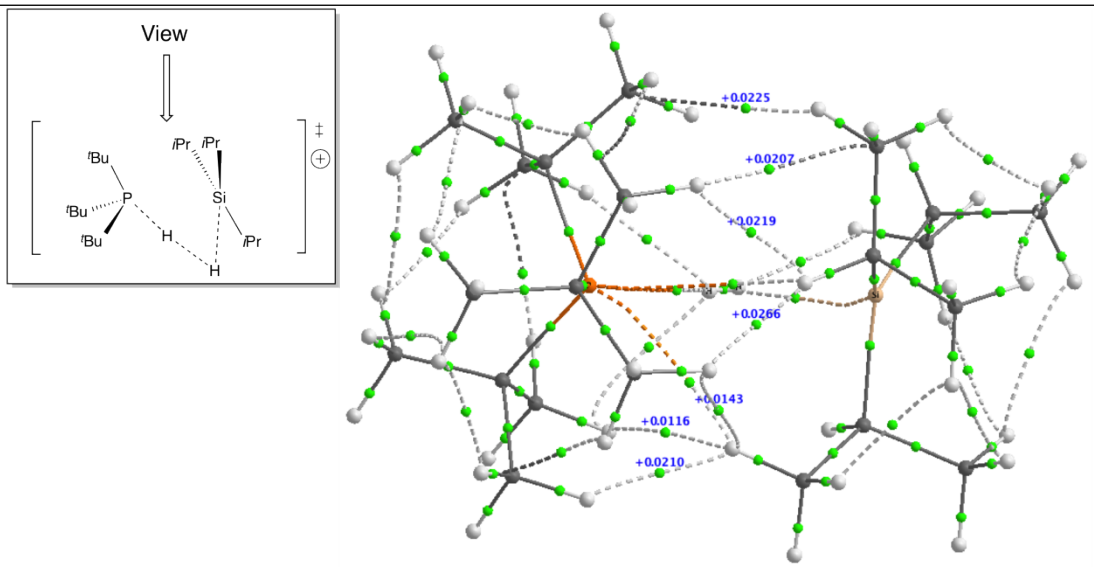

QTAIM analysis indicates the existence of several BCPs between the *t*Bu$_3$P and Si*i*Pr$_3$ fragments. Examination of the transition state from a side on view (Table S2) reveals the presence of two C–H···P interactions. These interactions have small, positive values associated with ρ(r) (0.0078 and 0.0081) and $\nabla^2\rho(r)$ (+0.0163 and +0.0169), consistent with weak van der Waals interactions.[12]

Adoption of a top-down view of the transition state (Table S4) reveals a number of C–H···H–C and C–H···C interactions. As with the C–H···P interactions, ρ(r) and $\nabla^2\rho(r)$ have small, positive associated values, again characteristic of weak van der Waals interactions. The summation of several weak van der Waals interactions between the *t*Bu$_3$P and Si*i*Pr$_3$ fragments contributes to the stabilisation of the transition state.

Table S5. Selected ρ(r) and $\nabla^2\rho(r)$ values (in a.u.) corresponding to P···H(H), Si···H(H) and C–H···H(H) interactions.

Viewing Orientation	Top Down
ρ(r)	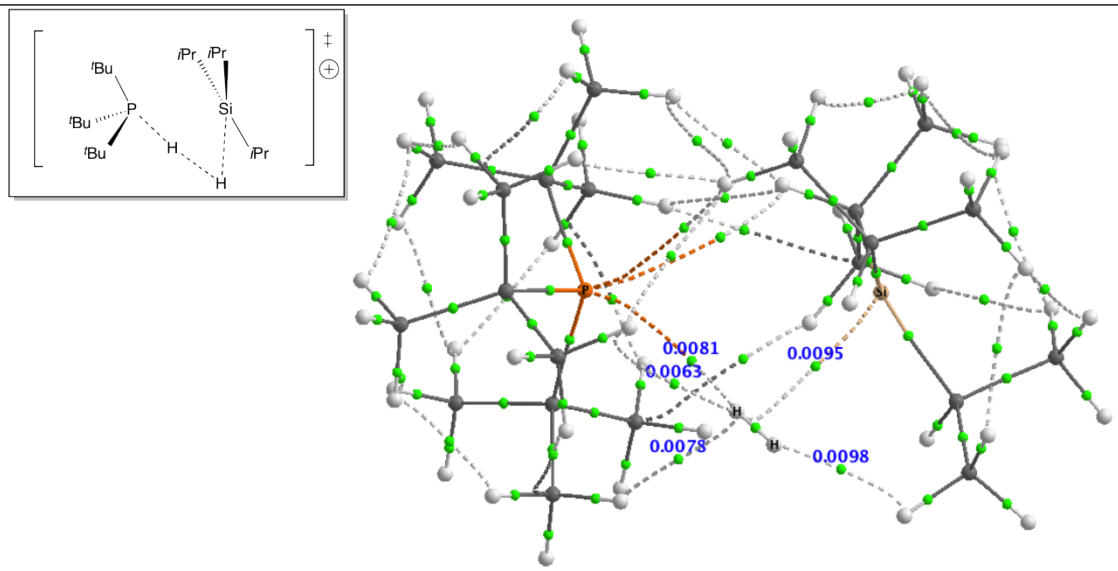
$\nabla^2\rho(r)$	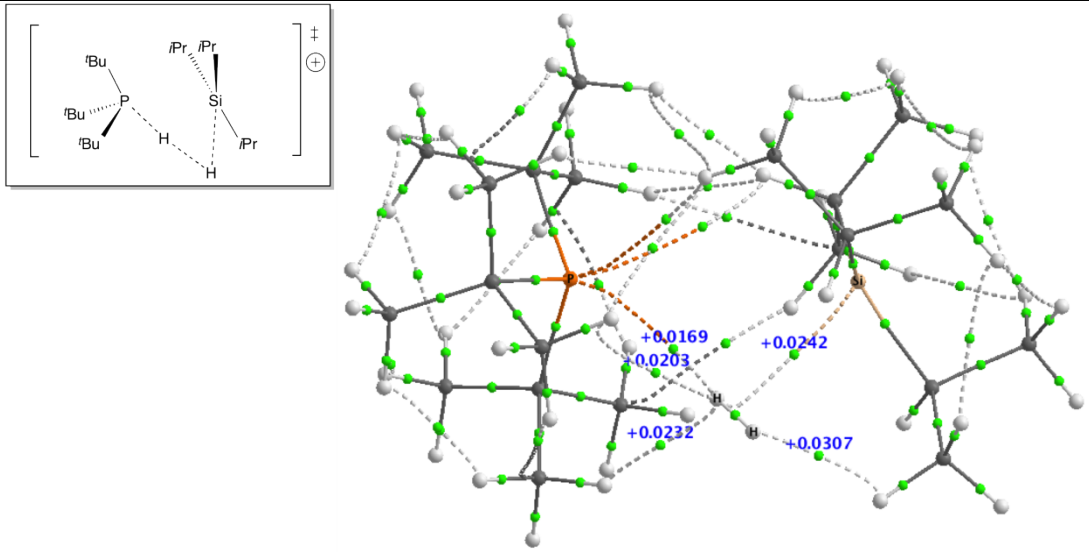

S13 References

1 R. C. Srivastava, *J. Chem. Res-S.* 1985, 330.

2 M. Lehmann, A. Schulz and A. Villinger, *Angew. Chem. Int. Ed.* 2009, **48,** 7444.

3 A. Schaefer, W. Saak, D. Haase and T. Mueller, *Angew. Chem. Int. Ed.,* 2012, **51**, 2981.

4 C. Wang, G. Erker, G. Kehr and R. Frölich, *Organometallics,* 2005, **24**, 4760.

5 M. Arisawa, T. Ichikawa and M. Yamaguchi, *Tetrahedron Lett.,* 2013, **54**, 4327.

6 M. J. Frisch, G. W. Trucks, H. B. Schlegel, G. E. Scuseria, M. A. Robb, J. R. Cheeseman, G. Scalmani, V. Barone, B. Mennucci, G. A. Petersson, H. Nakatsuji, M. Caricato, X. Li, H. P. Hratchian, A. F. Izmaylov, J. Bloino, G. Zheng, J. L. Sonnenberg, M. Hada, M. Ehara, K. Toyota, R. Fukuda, J. Hasegawa, M. Ishida, T. Nakajima, Y. Honda, O. Kitao, H. Nakai, T. Vreven, J. A. Montgomery, Jr., J. E. Peralta, F. Ogliaro, M. Bearpark, J. J. Heyd, E. Brothers, K. N. Kudin, V. N.

Staroverov, R. Kobayashi, J. Normand, K. Raghavachari, A. Rendell, J. C. Burant, S. S. Iyengar, J. Tomasi, M. Cossi, N. Rega, J. M. Millam, M. Klene, J. E. Knox, J. B. Cross, V. Bakken, C. Adamo, J. Jaramillo, R. Gomperts, R. E. Stratmann, O. Yazyev, A. J. Austin, R. Cammi, C. Pomelli, J. W. Ochterski, R. L. Martin, K. Morokuma, V. G. Zakrzewski, G. A. Voth, P. Salvador, J. J. Dannenberg, S. Dapprich, A. D. Daniels, Ö. Farkas, J. B. Foresman, J. V. Ortiz, J. Cioslowski and D. J. Fox, Gaussian 09, Revision B.01, Gaussian, Inc., Wallingford CT, **2009**.

7 Y. Zhao and D. G. Truhlar, *Theor. Chem. Acc.* 2008, **120**, 215.

8 S. Schirmer and S. Grimme, *Top. Curr. Chem*. 2013, **332**, 213.

9 K. Fukui, *Acc. Chem. Res.* 1981, **14**, 363; b) H. P. Hratchian and H. B. Schlegel, in *Theory and Applications of Computational Chemistry: The First 40 Years*, (Eds.: C. E. Dykstra, G. Frenking, K. S. Kim, G. Scuseria), Elsevier, Amsterdam, 2005, 195–1

10 (a) V. Barone and M. Cossi, *J. Phys. Chem. A* 1998, **102**, 1995; (b) M. Cossi, N. Rega, G. Scalmani and V. Barone, *J. Comput. Chem.* 2003, **24,** 669.

11 R. Dennington, T. Keith and J. Millam, GaussView, Version 5, *Semichem Inc.*, Shawnee Mission KS, 2009.

12 R. Parthasarathi, V. Subramanian and N. Sathyamurthy, *J. Phys. Chem. A.,* 2006, **110**, 3349.